Tôhoku Geophys. Journ. (Sci. Rep. Tôhoku Univ., Ser. 5), Vol. 31, No. 3, 4, pp. 57-99, 1988

Stress and Displacement Fields in the Northeastern Japan Island Arc as Evaluated with Three-Dimensional Finite Element Method and Their Tectonic Interpretations

KACHISHIGE SATO

International Latitude Observatory of Mizusawa,
Mizusawa, Iwate Pref. 023

(Received March 25, 1988)

Abstract: Numerical experiments for evaluation of the stress and displacement fields within the northeastern Japan island arc were performed by using three-dimensional finite element method. We study mainly the accumulation process of the stress within the arc by imposing boundary conditions as realistically as possible upon the plate-interaction models. Since this arc has very different structures in its southern and northern parts, calculations were separately made for these two parts. They roughly correspond to the Kanto and Tohoku districts, respectively.

The patterns of calculated vertical displacement fields at the earth's surface are generally similar to the observed ones in the models of both parts. As to the stress, in the southern part, it is large not only in the shallower portion of the thrust zone between the subducting and overriding plates, but also in the deeper portion where two subducting slabs collide beneath the land area. In the northern part, stress in the land area is nearly horizontally compressive and its axis is approximately in east-west. Furthermore, stresses in the upper crust increase with time more rapidly than those in the lower crust. The distribution pattern of large earthquakes off the Tohoku district can be interpreted by considering a spatial variation in the seismic-coupling between the subducting Pacific plate and overriding land side plate.

1. Introduction

Since the late 1960's, considerable progress has been made in the earth science with an innovative concept of the plate tectonics. A lot of geophysical and geodetic phenomena, such as earthquakes, crustal movement and so on, can be successfully interpreted with this concept in a general sense. In particular, in the case of the Japan island arc, many geophysical and geodetic phenomena have been considered in relation to the interactions among the continental plate(s) on which the Japan island arc exists and the oceanic plates, *i.e.*, the Pacific and Philippine Sea plates.

The Japan island arc is usually considered to be separable into five subarcs, namely, the Kurile, northeastern Japan, southwestern Japan, Ryukyu and Izu-Bonin island arcs (*e.g.* Uyeda and Sugimura, 1970). In the present study, only the northeastern Japan island arc is concerned with. Furthermore, we separate this arc into the southern and northern parts, which roughly correspond to the Kanto and Tohoku districts, respectively. As for the southern part, it is generally accepted that two oceanic plates, the Pacific

and Philippine-Sea plates, are underthrusting beneath the continental plate. Thus the underground structure beneath this region is rather complicated. On the other hand, the underground structure of the northern part is relatively simple. It is considered to be typical arc-trench system: only the Pacific plate is subducting under the continental plate. However, very recently, a new idea appeared that the easternmost part of the crust beneath the Japan Sea may be slightly underthrusting (*e.g.* Kobayashi, 1983; Nakamura, 1983). Anyway, the southern and northern parts of this arc are thus very different from each other in their structures. This is the reason why the parts are treated separately in this study.

As mentioned already, earthquake activities and crustal movement in these regions are considered to be the results of interactions among the plates. Therefore, it is not only very interesting but also very important from the viewpoint of earthquake prediction to evaluate numerically the stress and displacement fields caused by interactions among the plates and to interpret them by tectonics in these regions. Thus the purpose of the present study is to elucidate the tectonics in the northeastern Japan island arc and to give a certain basic suggestion for earthquale prediction.

2. Characteristics of Seismicity and Crustal Movement in the Northeastern Japan Island Arc

Intensive works which have been made so far in geodesy and geophysics have revealed some characteristics of seismicity and crustal movement in the northeastern Japan island arc. Herein, these characteristics are briefly summarized.

First, we look into the southern part. In this part, three plates meet together: two

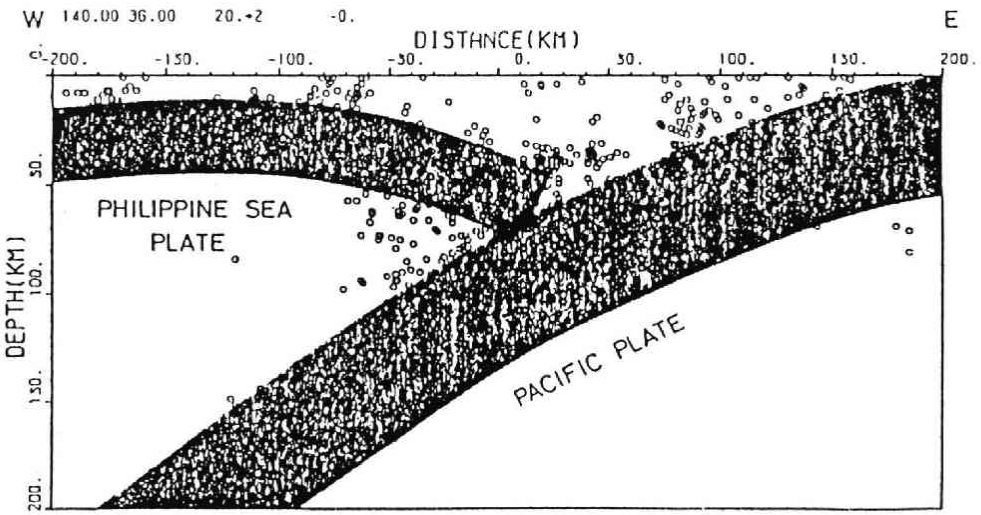

Fig. 1 East-West cross-section of hypocentral distribution of microearthquakes within a zone of 20 km in width centered upon a latitude line of 36°N. Interpreted configuration of the Pacific and Philippine-Sea plates is also shown (Ohtake and Kasahara, 1983).

oceanic plates, namely, the Pacific and Philippine-Sea plates, and one continental plate, the Eurasian plate (or the North-American plate). Thus it is frequently referred to as a region of triple junction.

Seismic activities in this region is considered as the results of interactions among these three plates (*e.g.* Maki *et al.*, 1980 ; Shimazaki *et al.*, 1982 ; Ohtake and Takahashi, 1982 ; Kasahara, 1985). According to the model presented by Kasahara (1985), the two oceanic plates are colliding with each other beneath the Kanto district, and major seismic activity is seen along the boundary of these oceanic plates. Ohtake and Kasahara (1983) investigated the seismicity in and around the Ibaraki prefecture. They showed an east-west cross section of hypocenter distribution of microearthquakes as presented in Fig. 1. In the figure, interpreted configuration of the Pacific and Philippine-Sea plates is also illustrated. It is clearly seen that so many earthquakes occur in and around the portion where two oceanic plates are colliding with each other. This pattern of seismicity is one of the most striking characteristics in this part.

On the other hand, in regard to the vertical crustal movement in this part, a subsidence in the northern portion of the Kanto plain is remarkable as shown in Fig. 2 (Dambara, 1971). This subsidence is called the Kanto basin building (*e.g.* Naruse, 1968).

Secondly, we inquire into the northern part. An epicenter distribution of shallow microearthquakes is presented in Fig. 3. (Hasegawa *et al.*, 1985). As clearly seen in the

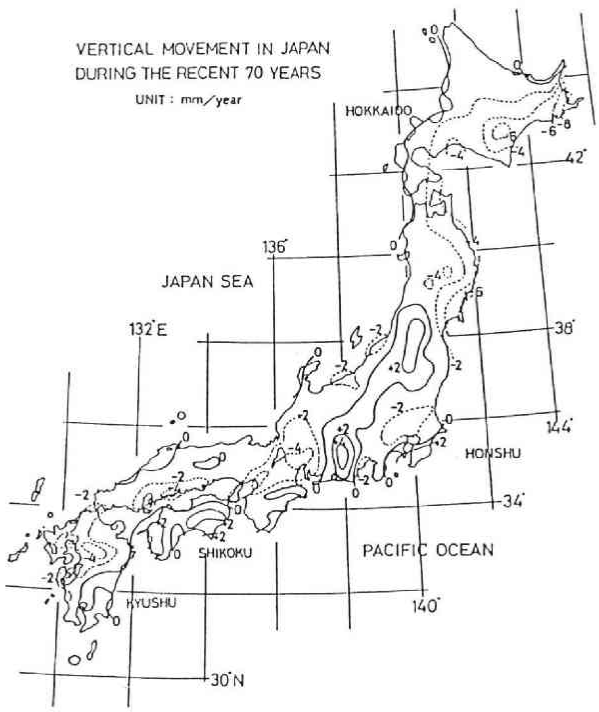

Fig. 2 Equal velocity contours of the vertical land movement within the Japan arc from 1895 to 1965 (Dambara, 1971).

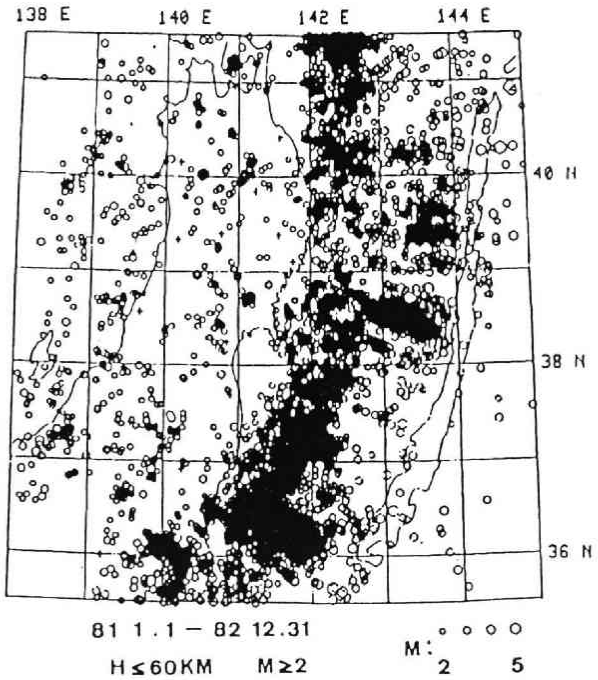

Fig. 3 Epicentral distribution of microearthquakes shallower than 60 km with a magnitude greater than 2 occurring in the period from January, 1982 to December, 1983 (Hasegawa *et al.*, 1985).

figure, most of shallow microearthquakes occur beneath the Pacific ocean between the Japan trench and the coastal line. The western margin of this belt-shaped zone where seismic activity is high is usually called the aseismic front (Yoshii, 1975). In the land area, a relatively high seismicity is notable along the so-called volcanic front which runs through the Honshu from north to south passing near the center of it. These shallow microearthquakes in the land area are confined to the upper crust as shown in Fig. 4 (Takagi *et al.*, 1977). A shallow seismic activity is also distinguished in the Japan Sea side of the Honshu.

On the other hand, one of the most important and interesting features of deep seismic activity beneath this part is its clear double-planed distribution pattern as shown in Fig. 5 (Umino and Hasegawa, 1975; Hasegawa *et al.*, 1978; Takagi, 1985). Furthermore, focal mechanisms of these earthquakes are systematically different among those in the upper and lower seismic planes, *i.e.*, down-dip compression type for the upper seismic plane and down-dip extension type for the lower one.

Next, we look into the pattern of large earthquake activities. Fig. 6 shows the aftershock area distribution for earthquakes with a magnitude greater than 7 occurring since 1926 in and around the northeastern Japan island arc (Hasegawa *et al.*, 1985). Large interplate earthquakes have frequently occurred beneath the Pacific ocean between the Japan trench and the Pacific coast similarly to the microearthquakes.

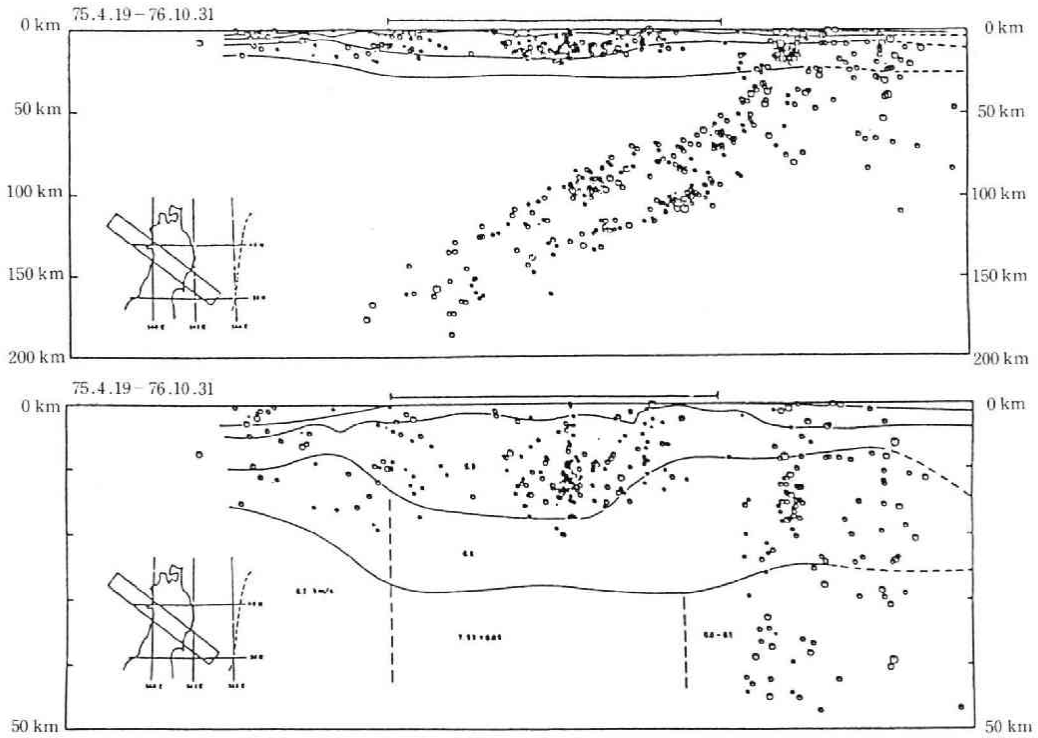

Fig. 4 Focal depth distribution of microearthquakes projected onto the vertical cross-section along the Kesen'numa-Oga profile, and the crust and uppermantle structures derived from explosion seismic observations by the Research Group for Explosion Seismology (1977) (Takagi *et al.*, 1977).

However, the distribution patterns of these large earthquakes are clearly different among those in the northern and southern areas bordered by a latitude line of about 38°N. In the northern area, large earthquakes occurred relatively near the trench axis, that is, far away from the coast. On the contrary, in the southern area, those are confined relatively near the coast. This is the most distinguishable fact with respect to the pattern of large earthquake activities in these areas. In addition to large earthquakes in the Pacific ocean side, a few large ones have occurred beneath the Japan Sea not so far away from the coast. Recently, a new hypothesis was proposed that there may be a nascent plate boundary at the easternmost portion of the Japan Sea basin (Kobayashi, 1983 ; Nakamura, 1983). Some of large events in the Japan Sea side may be related with this plate boundary (*e.g.* Mogi, 1985a, b).

As to the crustal movement in this part, Ishii *et al.* (1981) and Miura (1982) minutely investigated it. Fig. 7 shows the pattern of vertical movement given by Miura (1982). Among many characteristics, it is most striking that the Pacific ocean side of the Tohoku district subsides remarkably whereas the northern portion of the Japan Sea side slightly uplifts. Miura (1982) also noticed the existence of nodal points, or nodal line connecting them, in the vertical movement where no displacement occurs.

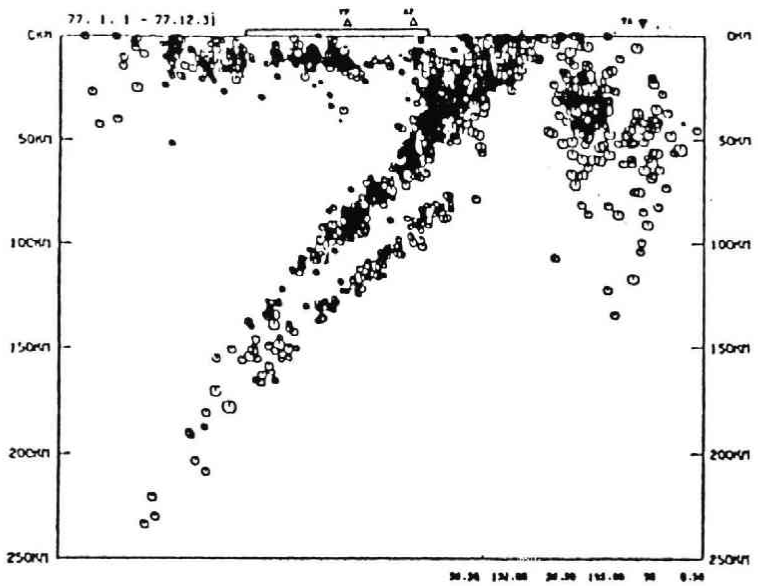

Fig. 5 Focal depth distribution of microearthquakes in the region from 39°N to 40°N projected onto a vertical cross-section in the E-W direction. Double-planed distribution pattern of deep quakes is obvious. 'TA', 'AF' and 'VF' denote the Japan trench axis, the aseismic and volcanic fronts, respectively (Takagi, 1985).

3. Method of Numerical Experiments

Three-dimensional finite element method for visco-elastic analysis were employed to calculate stress and displacement fields. There are a number of investigations adopting this method for such purpose (*e.g.* Jungels and Frazier, 1973; Bischke, 1974; Shimazaki, 1974; Kosloff, 1977; Bird, 1978; Kato, 1979; Seno, 1979; Sato, 1980; Minamino and Fujii, 1981; Hashimoto, 1984, 1985; Goto *et al.*, 1985). In the finite element method, complex boundary shapes and internal variations of material properties of continua are very easy to treat. The accuracy of solution with this method is generally satisfactory. This method, therefore, seems to be suitable to simulate the problems where heterogeneities and complex geometry are quite common.

General formulation of the finite element method is described in a number of excellent textbooks (*e.g.* Zienkiewicz, 1977; Togawa, 1979, 1981). As to the method of visco-elastic analysis, we adopted the one where supplementary parameters are used (Horii and Kawahara, 1970). In this method, a visco-elastic constitutive relation for a certain rheological model is expressed by using supplementary parameters which are to be eliminated. Time derivatives of strain are replaced by first difference approximations with assumption of constant strain rates in short periods. Thus giving the initial stress and strain, those at a time after a short period can be calculated. In the present study, the three-element model (standard linear solid) is adopted as a rheological model to represent the visco-elastic behavior of the earth (*e.g.* Kasahara, 1975). Complicated

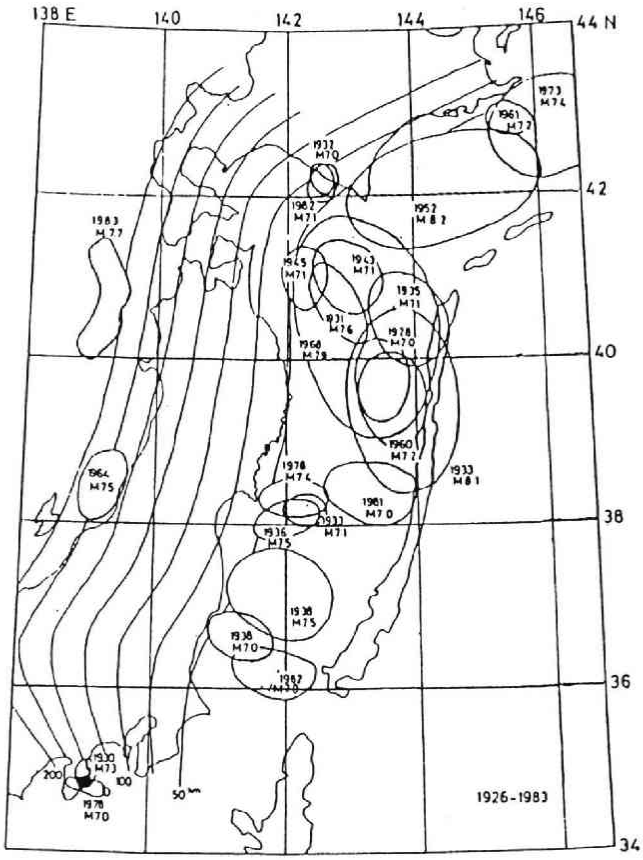

Fig. 6 Aftershock area distribution for events with magnitude greater than 7 occurring since 1926. Contour lines are those for iso-depth of the upper seismic plane (Hasegawa *et al.*, 1983).

rheological models are also easy to treat with this method. The accuracy of solution is generally satisfactory, if the time increment is taken to be short enough. In fact, the error of solution does not exceed 3% in test calculations by using simple models where the time increments are taken to be about one-tenth of the time constants of the models.

4. Finite Element Modeling of the Northeastern Japan Island Arc

4.1 Southern Part

4.1.1 Geometry and Material Properties

Many authors have so far presented the geometrical models of the two subducting oceanic plates beneath this part, *i.e.*, the Pacific and Philippine-Sea plates (*e.g.* Aoki, 1974; Maki, 1984; Noguchi, 1985; Kasahara, 1985; Ishida, 1986). These models are constructed based mainly upon the focal distributions of microearthquakes. They are consistent with one another in the gross. Hence we adopt the models given by Kasahara

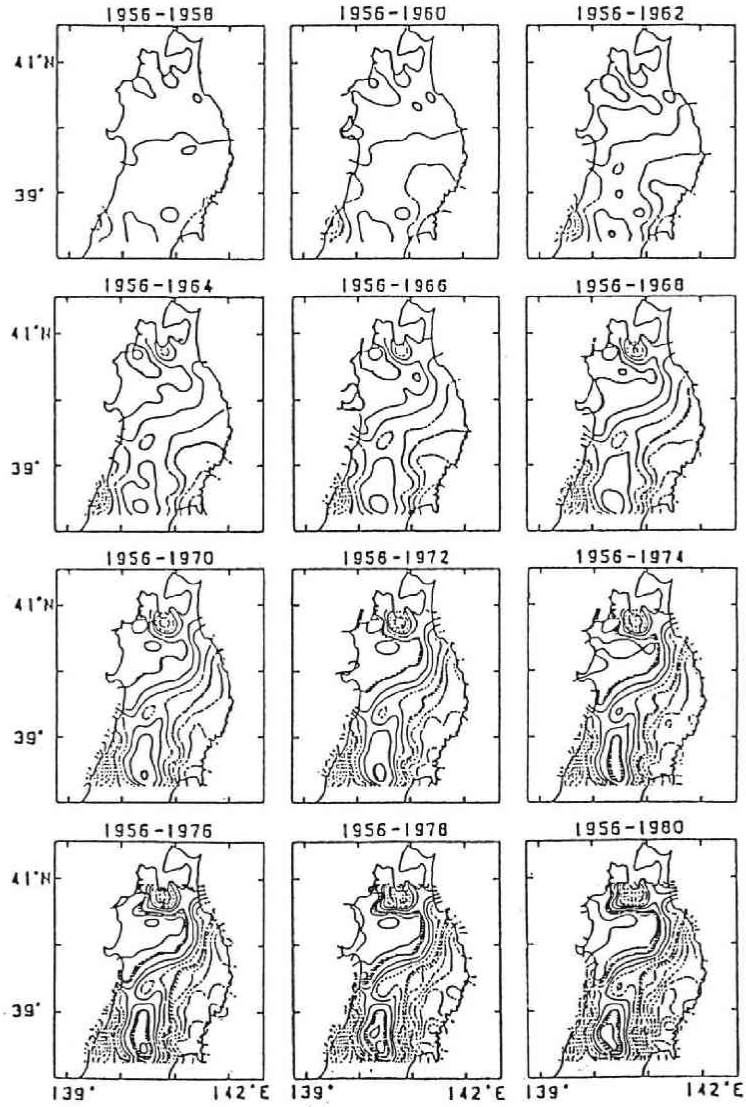

Fig. 7 Vertical movement in the Tohoku district from 1956 to 1980. Solid and dotted lines, respectively, denote uplift and subsidence. Contour intervals are 2 cm (Miura, 1982).

(1985) in the present study.

Fig. 8 shows the iso-depth contours of the upper surfaces of the Pacific and Philippine Sea plates given by Kasahara (1985). A three-dimensional model, which takes account of the geometry of these oceanic plates is constructed by using the iso-depth contours. We model a cubic region whose dimensions are 450 km in both of east-West and north-south directions and 400 km in depth. We neglect here both the curvature and topography of the earth's surface for simplicity. The origin of the coordinates

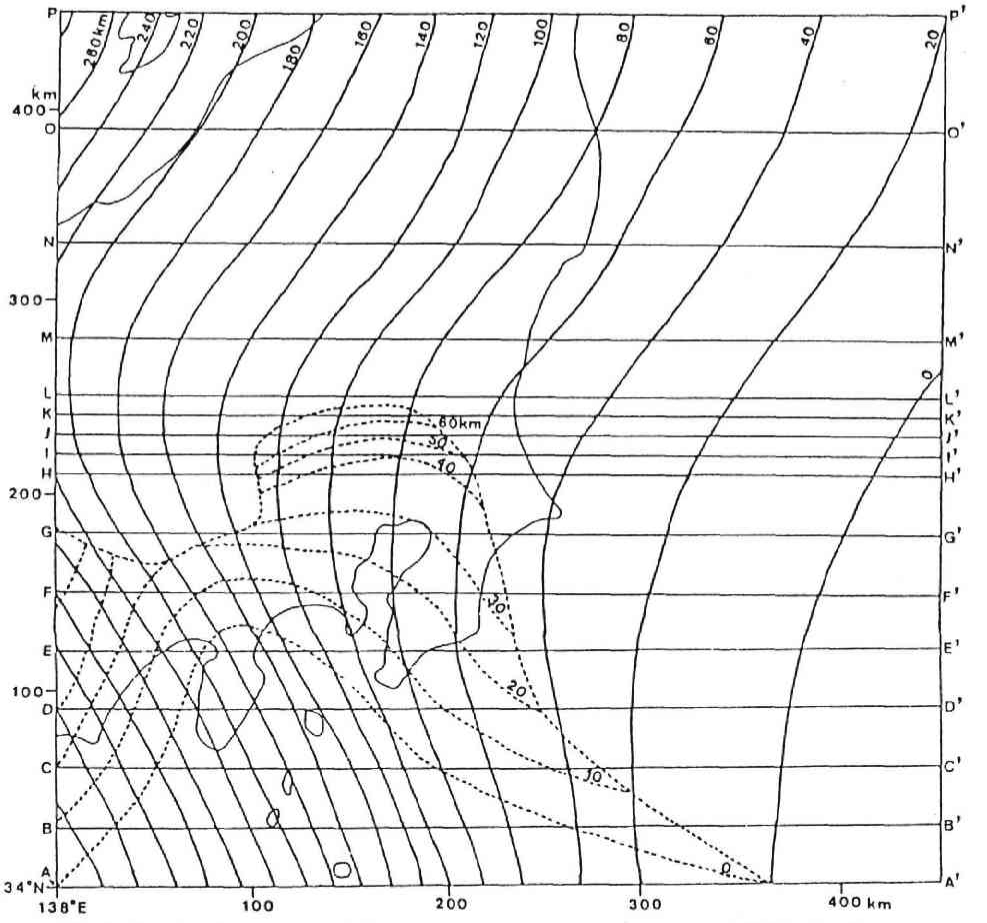

Fig. 8 Iso-depth contours of the upper surfaces of the Pacific and Philippine-Sea plates (in km) given by Kasahara (1985). The region is divided into slices by the segments from B-B′ to O-O′ as shown in this figure for the finite element modeling.

is set at the point (34°N, 138°E) on the earth's surface. A bird's-eye view of the model is shown in Fig. 9.

We divide the whole region into a number of hexahedral isoparametric finite elements, each of which has eight nodes on its apexes. First we slice the region along east-west direction with the segments (from B-B′ to O-O′) as shown in Fig. 8. The width of each slice is between 10 km and 60 km and it becomes narrower toward the central portion of the model. Next the profile of each vertical cross-section is drawn by using the iso-depth contours of the oceanic plates. The thicknesses of the Pacific and Philippine-Sea plates are assumed to be 60 km and 40 km, respectively. These thicknesses are almost the same as those derived by previous works (*e.g.* Kanamori and Press, 1970 ; Abe and Kanamori, 1970). The leading edge of the Philippine-Sea plate, however,

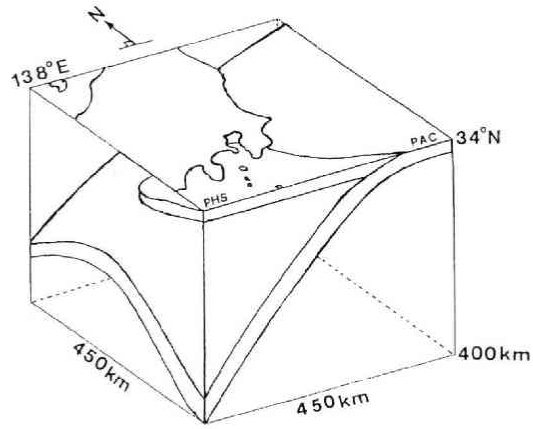

Fig. 9 A bird's-eye view showing the configuration of the southern part model.

is assumed to become gradually thinner toward its tip. Each of these cross-sections thus determined is divided into quadrilaterals. As an example, we show in Fig. 10(a) the cross-section along the segment E-E′ divided into quadrilateral meshes. Hexahedral finite elements can be made by connecting the quadrilaterals on adjacent cross-sections one by one. Thus a three-dimensional finite element model is constructed for the whole region shown in Fig. 9. The numbers of nodes and elements are 3648 and 3030, respectively, in this model.

We divide here the entire region into nine sub-regions according to their material properties as shown in Fig. 10(b). The physical parameters of the sub-regions are summarized in Table 1. We determined the parameters on the bases of those given by Sato *et al.* (1981) and Hashimoto (1984, 1985). The asthenosphere is assumed to be

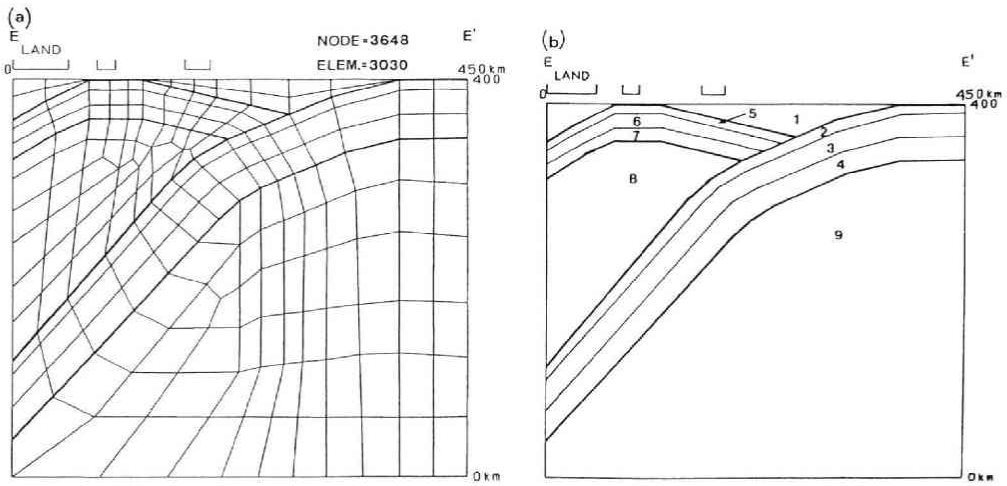

Fig. 10 The vertical cross-section along the segment E-E′ in Fig. 8 divided into quadribateral meshes (a) and sub-regions of different material properties (b).

Table 1. Material properties of the sub-regions in the southern part model. E, ν and η, respectively, mean the Young's modulus (in N/m^2), the Poisson's ratio and viscosity (in $N \cdot sec/m^2 = 10$ poise).

No.	E ($\times 10^{11}$)	ν	η ($\times 10^{13}$)
1	1.03	0.247	elastic
2	1.03	0.258	elastic
3	1.81	0.245	elastic
4	1.75	0.250	elastic
5	1.03	0.258	elastic
6	1.81	0.245	elastic
7	1.75	0.250	elastic
8	1.77	0.273	400
9	1.77	0.273	400

visco-elastic with a viscosity of 4×10^{21} $N \cdot sec/m^2$ (4×10^{22} poise). As mentioned previously, we adopt the three-element model (standard linear solid) as the rheological model to represent the visco-elastic behavior of the asthenosphere, since this model can interpret the crustal movement following the 1973 Nemuro-Oki Earthquake (Kasahara, 1975).

4.1.2 Boundary Conditions

We impose boundary conditions so that they can express as realistically as possible the plate-interactions, employing the plate motion models given by Seno (1977) and Minster and Jordan (1978, 1979). According to their models, the Pacific plate moves in a direction of about N70°W with a velocity of about 10 cm/yr, while the Philippine-Sea plate moves in a direction of about N55°W with a velocity of about 5 cm/yr. However, the net effects of these plates by dragging upon the overridng plate are assumed to be reduced to one-third by the existence of boundary layer between the plates. Such a reduction is suggested by Shimazaki (1974) and is also expected from the studies on the seismic-coupling between the subducting and overriding plates (*e.g.* Abe, 1977; Kanamori, 1977; Takemoto and Kawasaki, 1983; Kawasaki and Matsuda, 1987). Taking account of this reduction, we impose prescribed velocities upon the oceanic plates so that they express the motions caused by the slab-pull and ridge-push forces (Forsyth and Uyeda, 1975).

The earth's surface is treated as a free surface. All the nodes on model boundaries upon which no prescribed velocity is given are permitted only to slide on each boundary surface.

Since we consider only the deviatoric stresses, the gravitational force is not taken into account.

4.2 Northern Part

4.2.1 Geometry and Material Properties

Some authors have drawn the iso-depth contours of the deep seismic plane associated with the subduction of the Pacific plate beneath the northeastern Japan island arc (*e.g.* Hasegawa *et al.*, 1983). Here those given by Hasegawa *et al.* (1983) are adopted to make a geometrical model of the subducting Pacific plate (Fig. 11). We assume that the iso-depth contours of the upper seismic plane coincide with those of the upper surface of the Pacific plate.

According to Minster and Jordan (1978), the motion of the Pacific plate relative to the Eurasian plate has a direction of about N70°W in the vicinity of the northeastern Japan island arc. Since one of the boundary conditions should be imposed on in order to represent the relative motion of the Pacific plate, it is convenient to adopt a coordinate system where one of the coordinate axes coincides with this direction of relative plate motion.

Taking account of these points, we made three-dimensional model. The origin of

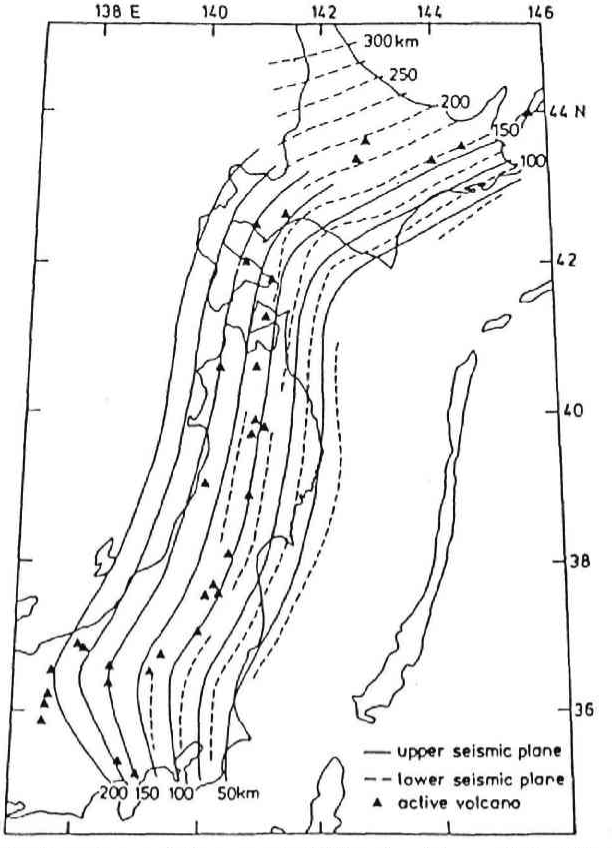

Fig. 11 Iso-depth contours of the upper (solid lines) and lower (dotted lines) seismic planes in the northeastern Japan island arc (Hasegawa *et al.*, 1983).

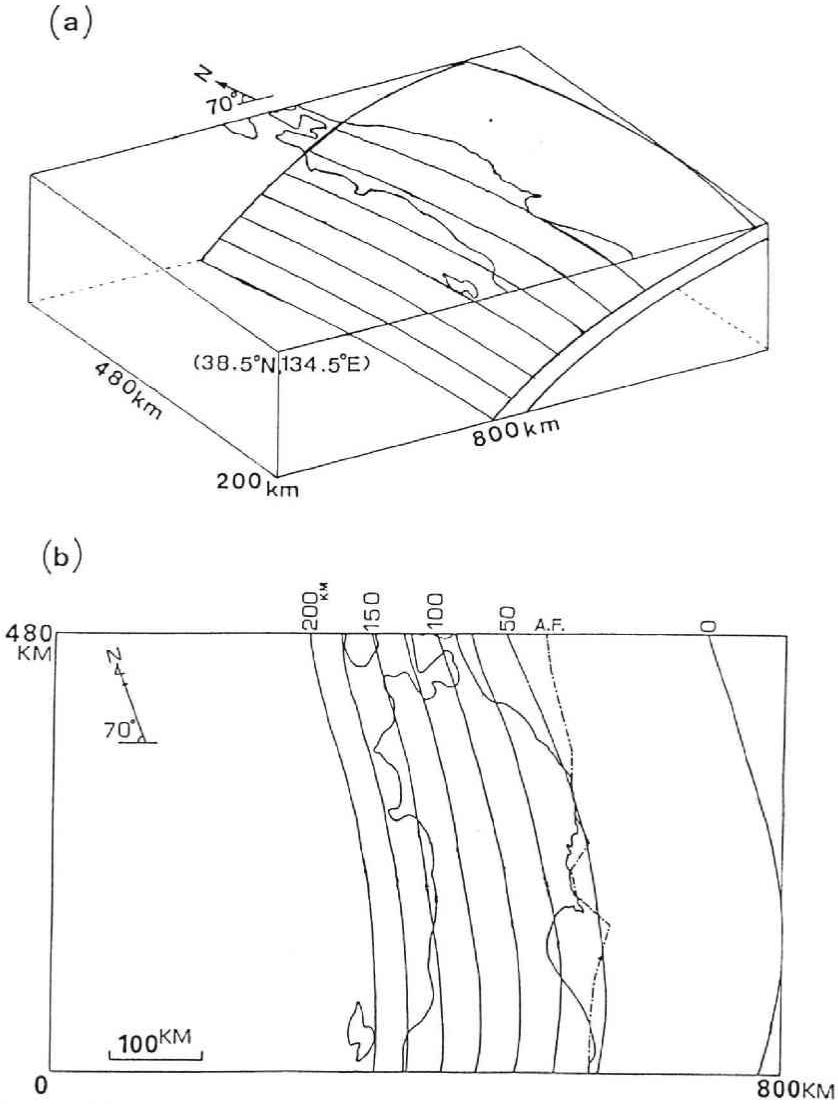

Fig. 12 A bird's-eye view showing the configuration of the northern part model (a) and its plane view (b). 'A.F.' means the aseismic front regarded in the present study (for detail see the text as well as Fig. 15). Solid curves are the iso-depth contours considered here of the upper surface of the Pacific plate.

the coordinate system is set at the point (38.5°N, 134.5°E) on the earth's surface, and the dimensions of the model are 800 km × 480 km in horizontal directions and 200 km in depth. Both the curvature and topography of the earth's surface are neglected as in the case of the southern part. Bird's-eye and plane views of the model are shown in Figs. 12(a) and (b), respectively.

In the case of the northern part model, our interests lie mainly in the stress and displacement fields within the crust and the upper mantle above the subducting Pacific

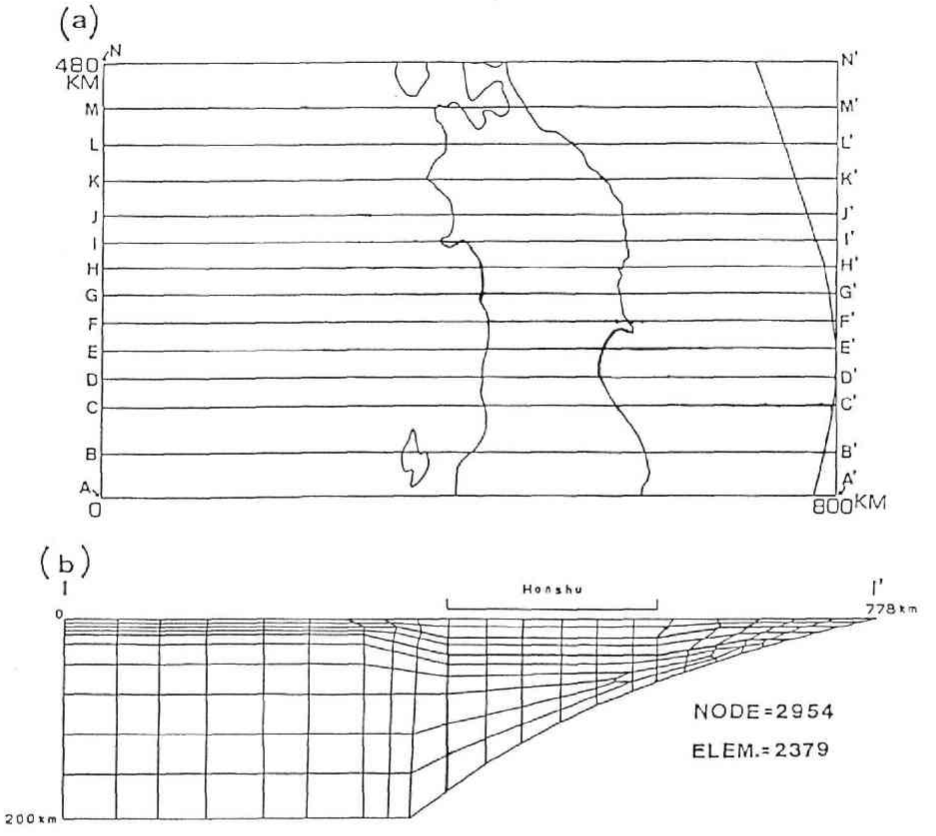

Fig. 13 Plane view of the northern part model divided into slices by segments from B-B′ to M-M′ (a) and its typical vertical cross-section along the segment I-I′ (b).

plate, *i.e.*, those within the overriding plate. Hence finite element model is constructed for the region above the interface between the subducting Pacific plate and overriding plate. The region is divided into hexahedral finite elements just as in the case of the southern part model. First we slice the whole region as shown in Fig. 13(a). Detailed cross-sectional view along the segment I-I′, for example, is illustrated in Fig. 13(b). The numbers of nodes and elements are 2954 and 2379, respectively, in this model.

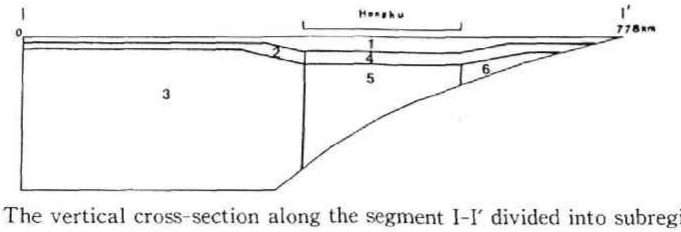

Fig. 14 The vertical cross-section along the segment I-I′ divided into subregions of different material properties.

Table 2. Material properties of the sub-regions in the northern part model. Meanings of E, ν and η are the same as in Table 1.

No.	E ($\times 10^{11}$)	ν	η ($\times 10^{13}$)
1	0.808	0.226	elastic
2	1.21	0.258	0.01
3	1.77	0.273	100
4	1.07	0.258	0.01
5	1.50	0.273	1
6	1.83	0.245	10

We divide the entire region into six sub-regions according to their material properties (Fig. 14). The physical parameters of the sub-regions are summarized in Table 2. We determined these parameters referring to the papers by Sato *et al.* (1981) and Hashimoto (1984, 1985).

4.2.2 Boundary Conditions

We give boundary conditions upon the surface representing the interface between

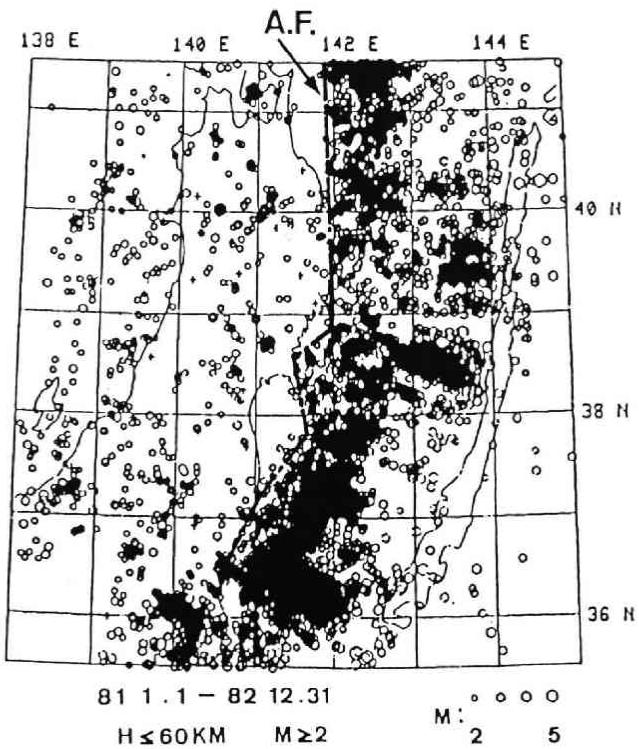

Fig. 15 The same as Fig. 3, but showing the aseismic front (solid line indicated by 'A.F.') regarded in the present study which is modified slightly from that of Yoshii (1975) (base map: Hasegawa *et al.*, 1985).

the subducting Pacific plate and overriding plate so that they express the interaction between these plates as realistically as possible. It is considered that the overriding plate is dragged downward by the subducting Pacific plate, because these two plates are partially coupled with each other on the interface from the Japan trench to some depth. In order to represent such dragged motion, prescribed displacements are imposed to the nodes on the interface shallower than a certain depth. These two plates are seemed to be coupled with each other from the trench axis to the depth just beneath the aseismic front (Sato, 1980 ; Miura, 1982). Hence we impose the prescribed displacements upon the nodes on the interface shallower than this depth. A horizontal projection of a line connecting the points of this depth adopted here is shown in Fig. 15 as the thick line indicated by 'AF' (aseismic front). The line is approximately coincides with the western margin of the active region in shallow seismicity. The horizontal projections of the prescribed displacements coincide with that of the motion of the Pacific plate relative to the Eurasian plate, that is, an N70°W direction. The prescribed displacements have only tangential components, so that they are parallel to the surface of the plate boundary.

With regard to the magnitudes of the prescribed displacements, two cases are considered, namely uniform-and variable-magnitude displacements. In the case of uniform-magnitude displacements, we uniformly impose upon all nodes the displacements increasing by 3 cm in every year. This rate is determined in the same way as the southern part model by considering the velocity of the Pacific plate and the strength of the seismic-coupling between the land side plate and this plate on their interface. As described previously, the strength of this seismic-coupling (hereafter we will refer to this as the seismic-coupling factor) around the Japan island arc is considered about 0.3 (*e.g.* Abe, 1977 ; Kanamori, 1977 ; Takemoto and Kawasaki, 1983 ; Kawasaki and Matsuda, 1987). This means that the displacements of the overriding plates at the plate interfaces which are caused by dragging by the subducting plates are about 30% of those associated with the plate motions themselves. Since the rate of the relative motion between the Pacific and Eurasian plates is about 10 cm/yr (Minster and Jordan, 1978), we give the displacement rates of 3 cm/yr. Hereafter we will refer to this as the constant-coupling case.

In above case, the seismic-coupling factor is regarded as constant over the entire region of the coupled surface. It is, however, natural to consider some variability in this factor with depth along the interface. Furthermore, it may vary regionally because, as shown in Fig. 6, the distribution patterns of large earthquakes off the Pacific coast are obviously different between those in the northern and southern areas bordered by a latitude line of about 38°N. In the strong coupling region, large earthquakes tend to occur frequently, whereas in the weak coupling region, they would not occur. Thus we consider other cases where the prescribed displacements have different magnitudes according to the variation in the seismic-coupling factor. We consider two functions representing the variations of this factor as shown in Figs. 16(a) and (b). In these figures, normalized seismic-coupling factors (C_F) are illustrated, which are defined as the ratio of the factor to its mean value, *i.e.*, 30% In the case of Fig. 16(a) (we will refer to this case

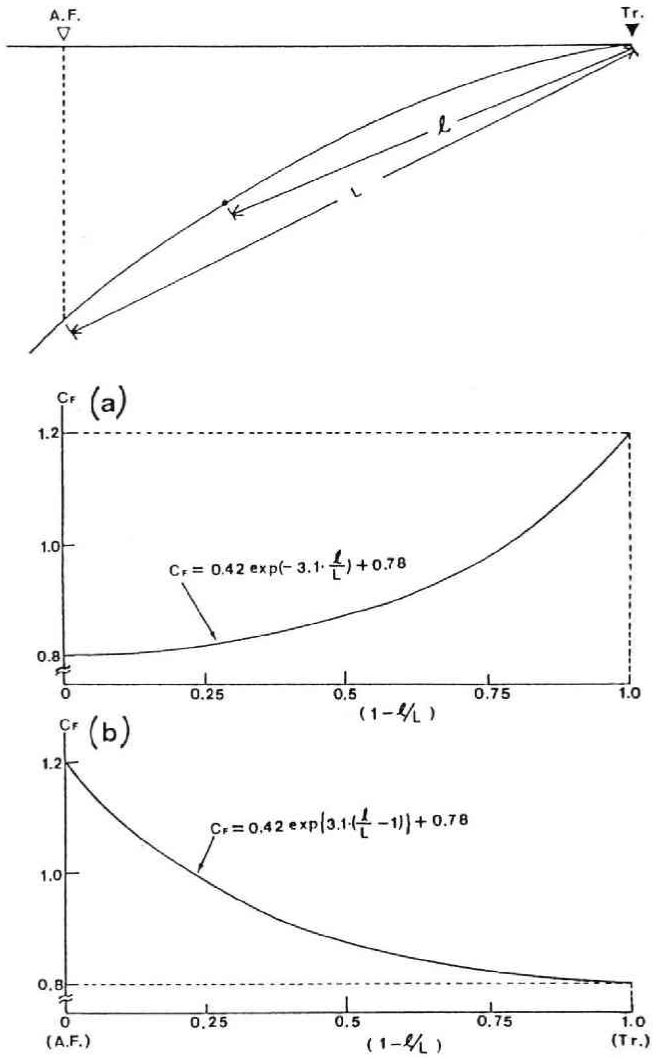

Fig. 16 Magnitude-distance relations for the normalized seismic coupling factor used in the case-(a) (a) and case-(b) (b), respectively. 'Tr.' and 'A.F.' in the uppermost illustration mean the Japan trench axis and the aseismic front, respectively.

as case-(a)), the normalized seismic-coupling factor is represented by

$$C_F = 0.42 \cdot \exp(-3.1 \cdot l/L) + 0.78, \tag{1}$$

whereas, in the case of Fig. 16(b) (we will refer to this case as case-(b)), it is represented by

$$C_F = 0.42 \cdot \exp\{3.1 \cdot (l/L - 1)\} + 0.78, \tag{2}$$

where L and l, respectively, mean the distances along the interface from the trench axis

to the position just beneath the aseismic front and to a point between them. In these cases, C_F varies from about 0.8 to 1.2. In other words, the seismic-coupling factor changes from about 24% to 36%. In practice, the magnitude of the prescribed displacement rate given to each node is represented by the product $3.0 \times C_F$ cm/yr. The larger the seismiccoupling factor is, of course, the stronger the coupling is. Therefore, in the case-(a), the coupling is strongest near the trench axis and becomes weaker with the distance from the trench axis or with the depth. On the contrary, in the case-(b), it is weakest near the trench axis and becomes stronger with the distance from the trench axis or with the depth. It is considered that the case-(a) and case-(b), respectively, correspond to the cases in the northern and southern areas bordered by a latitude line of about 38°N. We impose upon the nodes such prescribed displacements as those in the case-(a) and case-(b). Furthermore, we consider another case by combining the case-(a) and case-(b), where the seismic-coupling factor for the case-(a) and case-(b), respetively, applied to the northern and southern areas. This case will be referred to as case-(c).

In each case, the earth's surface and the remaining part of the plate interface between the Pacific plate and overriding plate are treated as free surfaces. All nodes on other model boundaries are constrained only to slide on each boundary surface.

The gravitational force is not taken into account in this model due to the same reason as in the case of the southern part model.

5. Results of Numerical Experiments and Their Tectonic Interpretations

Numerical computations of the stress and displacement fields in the northeastern Japan island arc were made with the models described in the preceeding section. The time increment between successive time steps in visco-elastic analysis was taken to be 20 years throughout these computations. The stress and displacement fields were calculated for four time steps, which span 60 years.

5.1 Results and Their Tectonic Interpretations for the Southern Part

5.1.1 Displacement Field

Horizontal displacement vectors and iso-magnitude contours of vertical displacement on the earth's surface at 60 years are illustrated in Figs. 17(a) and (b), respectively.

It is clearly seen in Fig. 17(a) that the pattern of the horizontal displacements on the surface is much affected by the motions of both the Pacific and Philippine-Sea plates, although the directions of the displacements are slightly different from each other in the eastern and western portions. The directions of the horizontal displacements in the eastern portion are almost coincident with the direction of the motion of the Pacific plate, that is, west or northwest direction. On the other hand, those in the western portion are almost the same as that of the Philippine-Sea plate, that is, north or northwest direction. The magnitudes of the displacements become smaller and smaller as they come toward west or northwest.

As to the vertical displacement shown in Fig. 17(b), it is most remarkable that the northern portion of the Kanto plain is subsiding. The magnitude of this subsidence

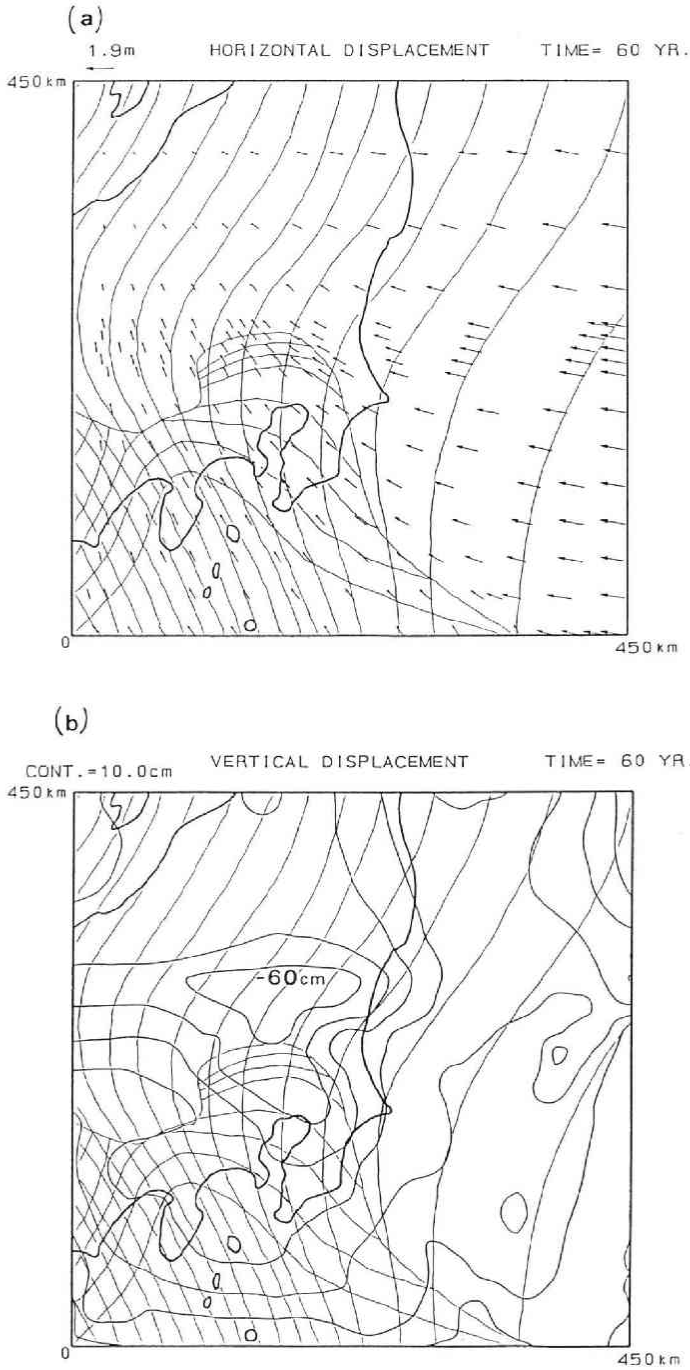

Fig. 17 Horizontal displacement vectors (a) and iso-magnitude contours of vertical displacement (b) on the earth's surface at the time of 60 years obtained for the southern part model. Thin curves denote the iso-depth contours of the upper surfaces of the Pacific and Philippine-Sea plates.

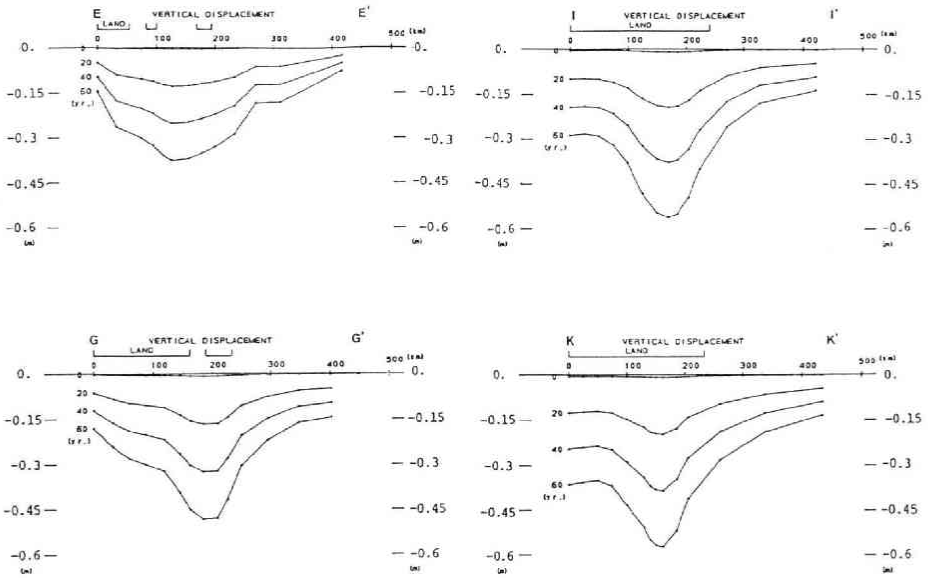

Fig. 18 Profiles of the vertical displacement on the earth's surface along the segments E-E', G-G', I-I' and K-K' in Fig. 8. Profiles for every 20 years are shown.

reaches 60 cm or more in 60 years. This means a subsidence rate of 1 cm/yr or more. The center of the subsiding portion is located at the place just north of the leading edge of the subducting Philippine-Sea plate.

Profiles of the vertical displacements are shown in Fig. 18, for example, along the cross-sections E-E', G-G', I-I' and K-K' with were indicated in Fig. 8. In this figure, the subsidence in the central portion of each crosssection is remarkable. The subsidence like this is also notable in the pattern of observed vertical movement which was presented in Fig. 2 (Dambara, 1971). The rate of the observed subsidence is about 2 mm/yr, which is only one-fifth of that of the calculated subsidence. Although this discrepancy in the subsiding rate between observation and calculation may be large (on this point we will discuss later), the patterns of observed and calculated vertical movements remarkably resemble each other.

We may be able to educe the cause of the observed subsidence by considering what the main origin of the calculated subsidence in numerical experiment is. The center of the subsiding portion in the calculated vertical displacement field is, as already mentioned, just at the north of the leading edge of the subducting Philippine-Sea plate and is very close to this edge. Thus it is quite reasonable to regard that the subsidence is caused mainly by the subduction of this oceanic plate. Kasahara (1985) also pointed out that the subsidence, which is commonly known as the Kanto basin building (*e.g.* Naruse, 1968), is possibly caused by the subduction of the Philippine-Sea plate whose leading portion beneath the subsiding region is continuously stripped off by the Pacific plate. Thus the predominant pattern of the vertical displacement field in the southern

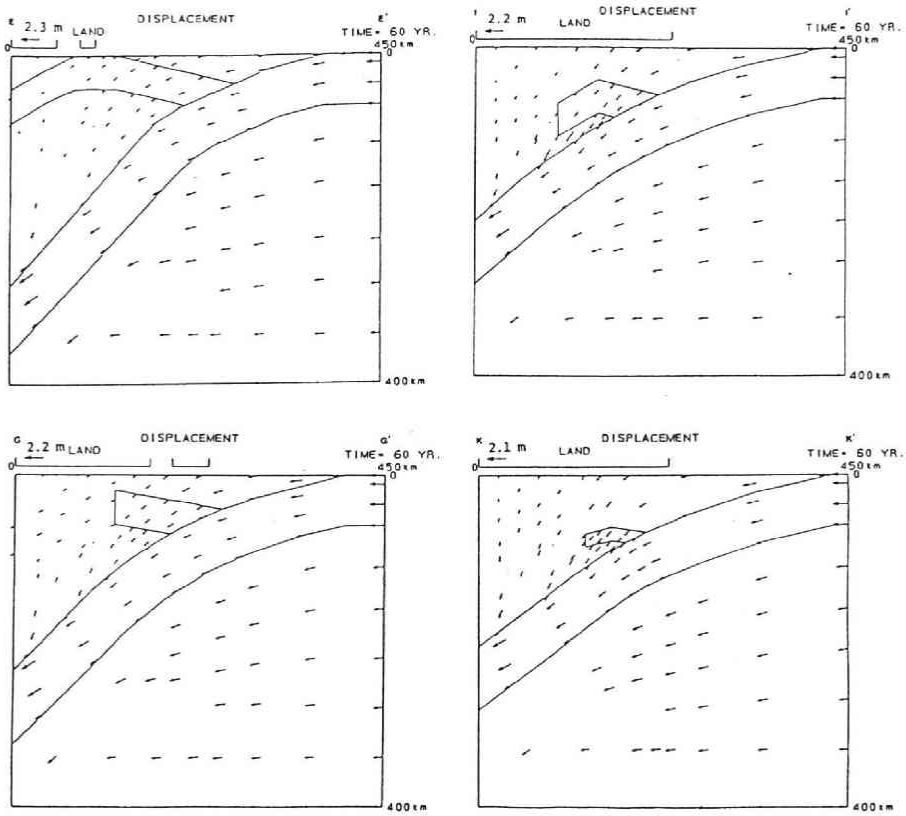

Fig. 19 Displacement vectors at 60 years on the vertical cross-sections along the segments E-E′, G-G′, I-I′ and K-K′ in Fig. 8. Configuration of the Pacific and Philippine-Sea plates is also shown.

part of the northeastern Japan island arc is considered to be caused by subduction of the Philippine-Sea plate.

Next the displacement vectors in the cross-sections, for example, E-E′, G-G′, I-I′ and K-K′ are illustrated in Fig. 19 for the time step of 60 years. The displacements caused by subduction of the Pacific plate are predominant in all cross-sections. The trends of displacement vectors are, however, slightly different from each other among the regions beneath and above the Pacific plate. Those in the region beneath this plate are almost parallel to the motion of the plate, whereas those in the region above the plate are somewhat downward. The difference in the trends of displacement vectors is, however, possibly an artificial one to some extent originated from boundary conditions.

5.1.2 Stress Field

Three-dimensional expressions of stresses in the crust and in the portion just along the plate interface between the Pacific plate and overriding plate, respectively, are shown in Figs. 20(a) and (b) as projections on the earth's surface. In these figures, size of each circle is in proportion to the magnitude of maximum shear stress and the shaded and

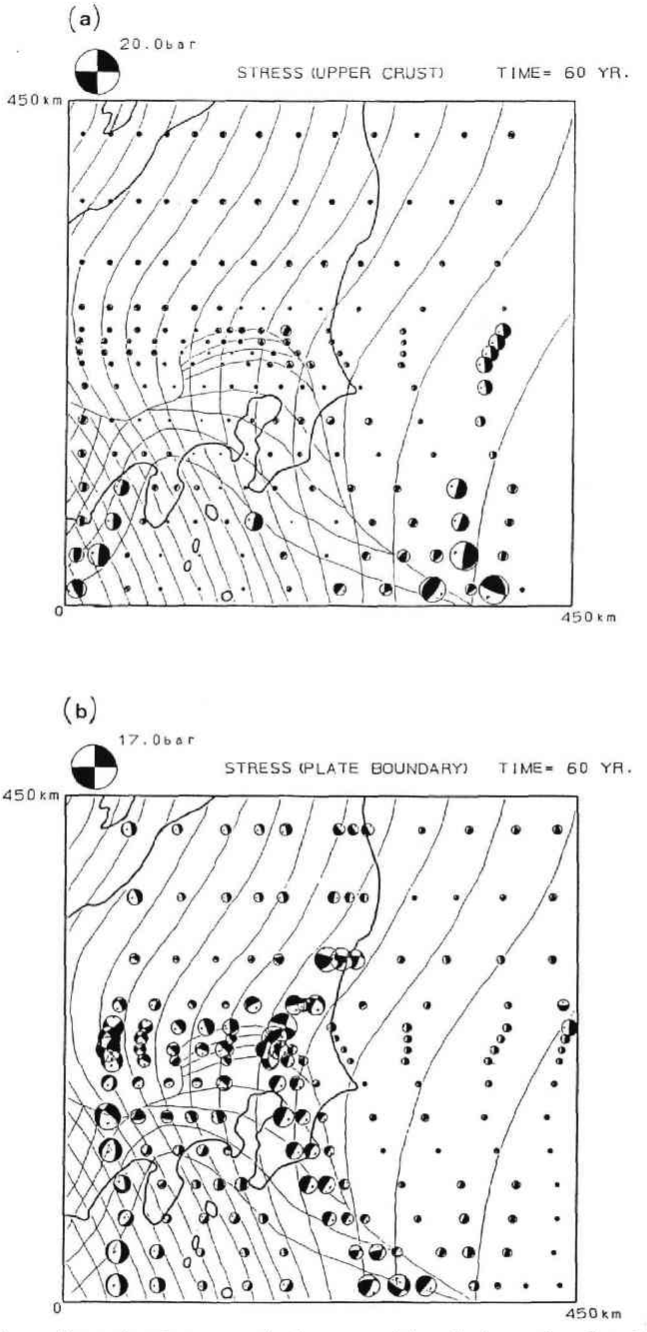

Fig. 20 Three-dimensional stresses in the crust (a) and along the plate boundary between the Pacific plate and overriding plate (b) at the time of 60 years. Stresses are the lower hemisphere projections, and the sizes of circles are in proportion to the maximum shear stresses. Shaded parts are tensile, which correspond to those of compressional first motion. Open parts are compressional. The letters 'P' in the open parts mean the compressional axes.

open portions in each circle, respectively, represent tensional and compressional quadrants projected on the lower hemisphere. The letters 'P' in the open portions denote the compressional axes.

Regarding the stress distribution in the crust, several regions where the stresses are large should be noted. Those are the regions near the Suruga trough, in and around the so-called triple junction located off the Boso peninsula, and far offshore the Ibaraki prefecture. In these regions, downdip compressional fields of stress are revealed. In the northern portion of the Kanto plain, where a remarkable subsidence appears, the stresses are also relatively large. The stresses in the northern half of the analyzed region are almost homogeneous both in magnitudes of the maximum shear stresses and in orientations of principal axes. The stress field in land is horizontally compressional in general, so that reverse type faulting tends to occur. The directions of compressional axes are nearly consistent with those summarized by Tsukahara and Ikeda (1983) except

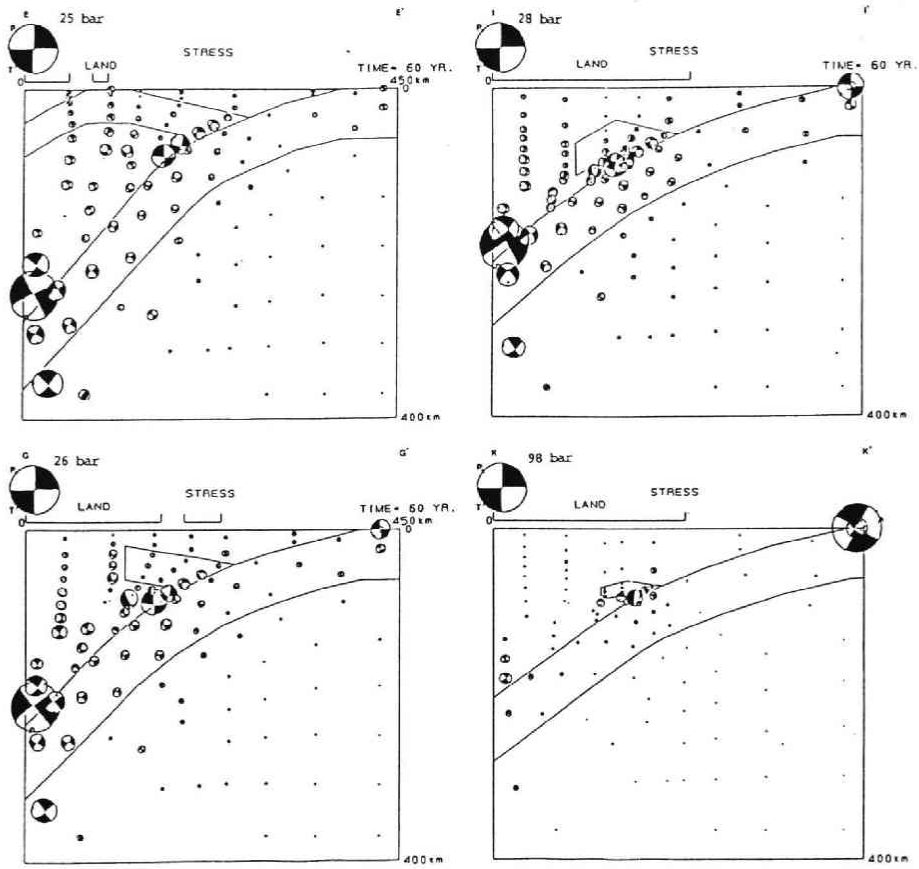

Fig. 21 Stresses at 60 years projected onto the front hemispheres in the vertical cross-sections along the segments E-E', G-G', I-I' and K-K' in Fig. 8. Notations are the same as in Fig. 20. Configuration of the Pacific and Philippine-Sea plates is also shown.

for those in and around the Izu peninsula.

Next, in the stress distribution along the interface of the Pacific plate, the stresses in and around the zone where the slabs of two oceanic plates meet together are predominantly large. The stresses in the portion near the leading edge of the Philippine-Sea plate are especially large. The compressional axes of the stresses in this portion are nearly perpendicular to the surface of the Pacific plate except those in the southern region.

Cross-sectional distributions of stresses are shown in Fig. 21 for the segments, for example, along E-E′, G-G′, I-I′ and K-K′ shown in Fig. 8. In these figures, the quadrants of tension and compression are projected, in this time, on the front hemisphere. The same expressions will be used hereafter for illustrating the cross-sectional distributions of stresses. In these cross-sectional views, the stresses in and around the portions where the slabs of the Pacific and Philippine-Sea plates are colliding each other are also found to be large and to have compressional axes almost perpendicular to the surface of the interface between these two slabs. Such orientation of the compressional axis of stress is consistent to a considerable extent with the source mechanisms of earthquakes occurring in this region (*e.g.* Ohtake and Kasahara, 1983).

5.2 Results and Their Tectonic Interpretations for the Northern Part

5.2.1 Displacement Field

First we look into the displacement fields on the earth's surface. Shown in Figs. 22(a) and (b), respectively, are horizontal displacement vectors and iso-magnitude contours of vertical displacement in the case of the constant seismic-coupling. These are the displacements at 60 years. The horizontal displacement vectors are almost parallel to one another and have the same direction as that of the motion of the Pacific plate. Magnitude of the horizontal displacement decreases with distance from the trench axis. The displacement at the portion far off the Japan Sea coast is very small. The horizontal displacement in the land area is about 110 cm : the rate of horizontal displacement is about 1.8 cm/yr. This is of the same order as those obtained by observations (Harada and Isawa, 1969).

As regards the vertical displacement, the iso-magnitude contours in the land area are almost parallel to one another and approximately in the direction from NNE to SSW, which is the direction crossing with a slightly oblique angle the iso-depth contours of the subducting Pacific plate or the strike of the island arc. General feature of the pattern in the vertical displacement field is similar to that obtained by observations (*e.g.* Dambara, 1971 ; Kato, 1979 ; Ishii *et al.*, 1981 ; Miura, 1982) and to that obtained by previous simulations (*e.g.* Sato, 1980 ; Miura, 1982). The contour line of zero vertical displacement runs fror north to south near the Japan Sea coast. The position of this line is, however, somewhat westerly as compared with the one obtained by Miura (1982). The difference may arise from the difference in simulation model, that is, those in the dip angle of the subducting Pacific plate and/or in the position of the western extremity of the coupling interface between the subducting and overriding plates. Eastern and

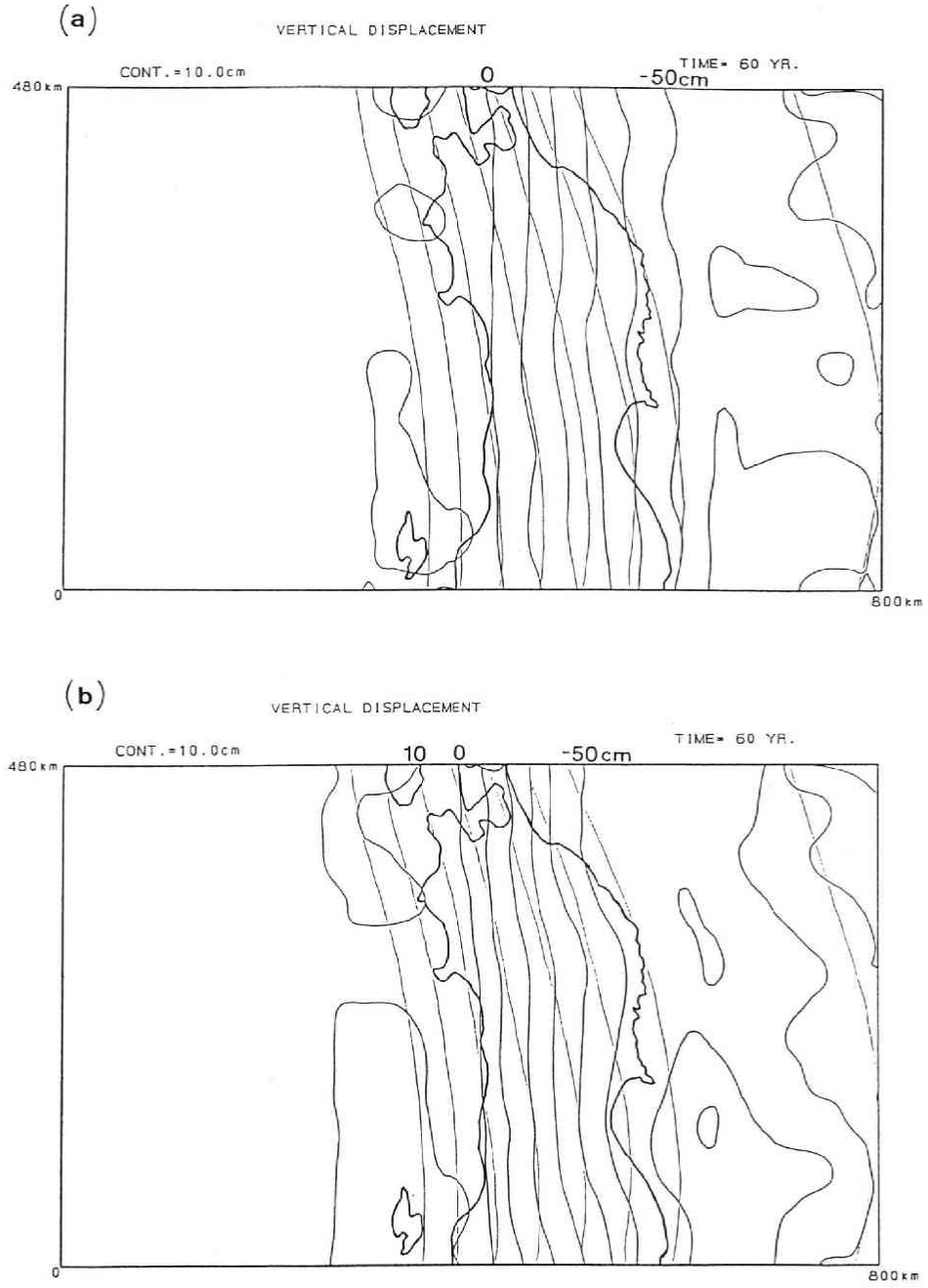

Fig. 22 The same as Fig. 17(a) and (b), but for the northern part model in the costant-coupling case.

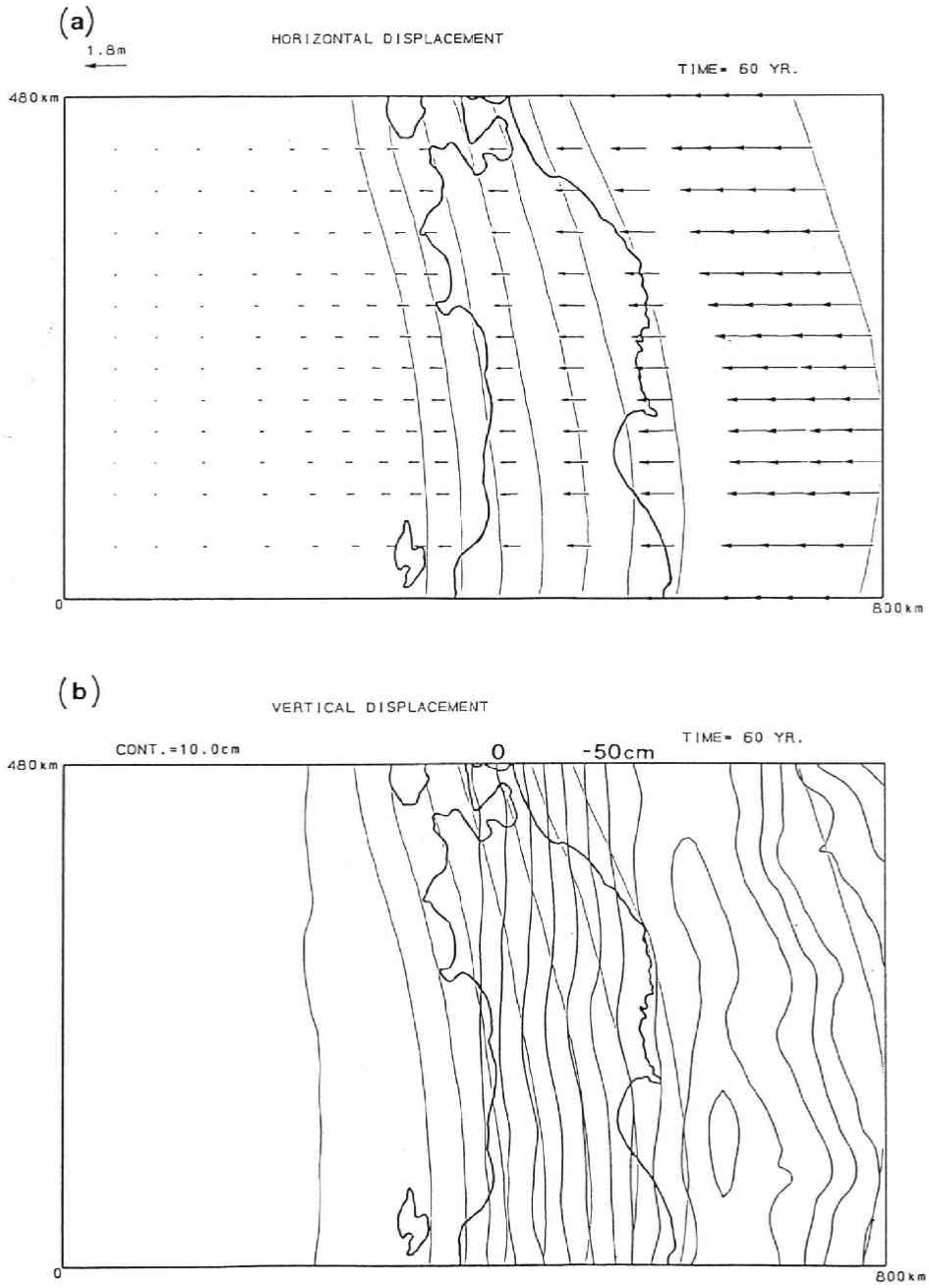

Fig. 23 Iso-magnitude contours of vertical displacements on the earth's surface at the time of 60 years obtained for the northern part model in the case-(a) (a) and case-(b) (b), respectively.

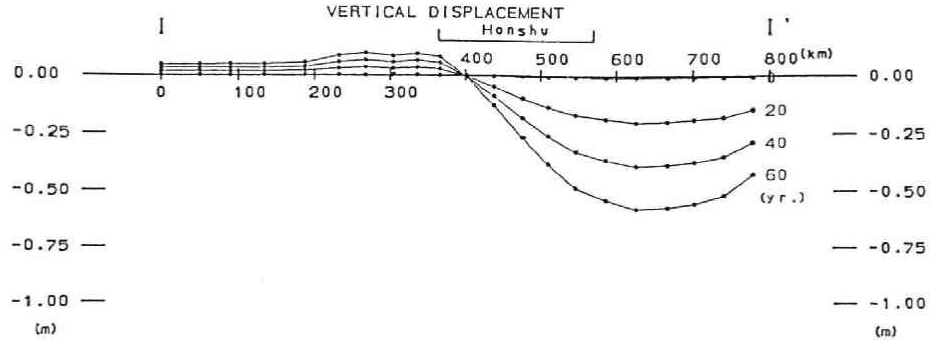

Fig. 24 The same as Fig. 18, but for the northern part model in the constant-coupling case. This profile is along the segment I-I' in Fig. 13(a).

western sides of the nodal line are subsiding and uplifting, respectively. Most portion near the Pacific coast subsides more than 50 cm in 60 years. Thus the subsidence rate is about 8 mm/yr, which is a few times larger than the observed one (Dambara, 1971 : see Fig. 2).

As shown in Figs. 23(a) and (b), patterns of the contour lines in the land area are similar to one another, even if the prescribed displacements given to the coupling interface are changed as in the case-(a) and case-(b). The position of each contour lines, however, varies slightly. The spacing of contour lines becomes wide and narrow, respectively, in the case-(a) and case-(b), so that the Pacific coast nearly coincides with the contour line of -40 cm in the case-(a) and with that of -60 cm in the case-(b),

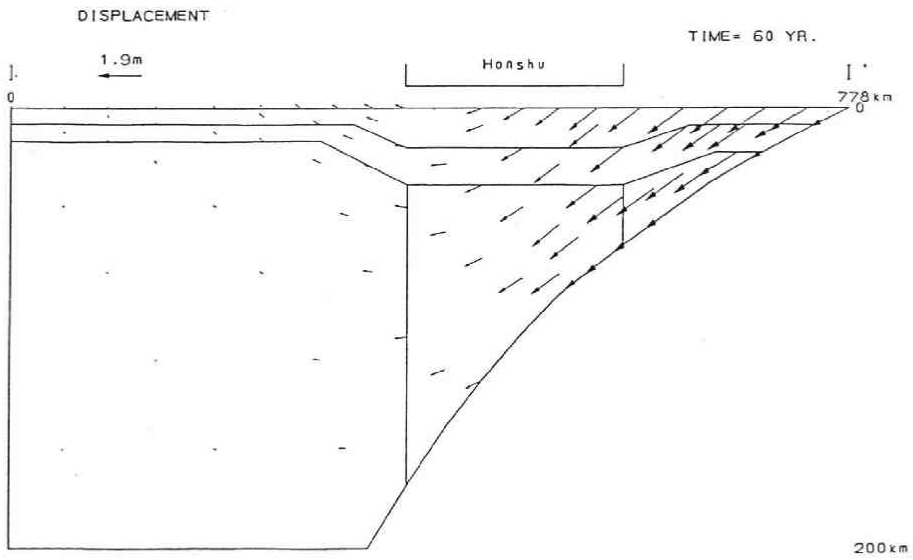

Fig. 25 The same as Fig. 19, but for the northern part model in the constant-coupling case. This cross-section is along the segment I-I' in Fig. 13(a).

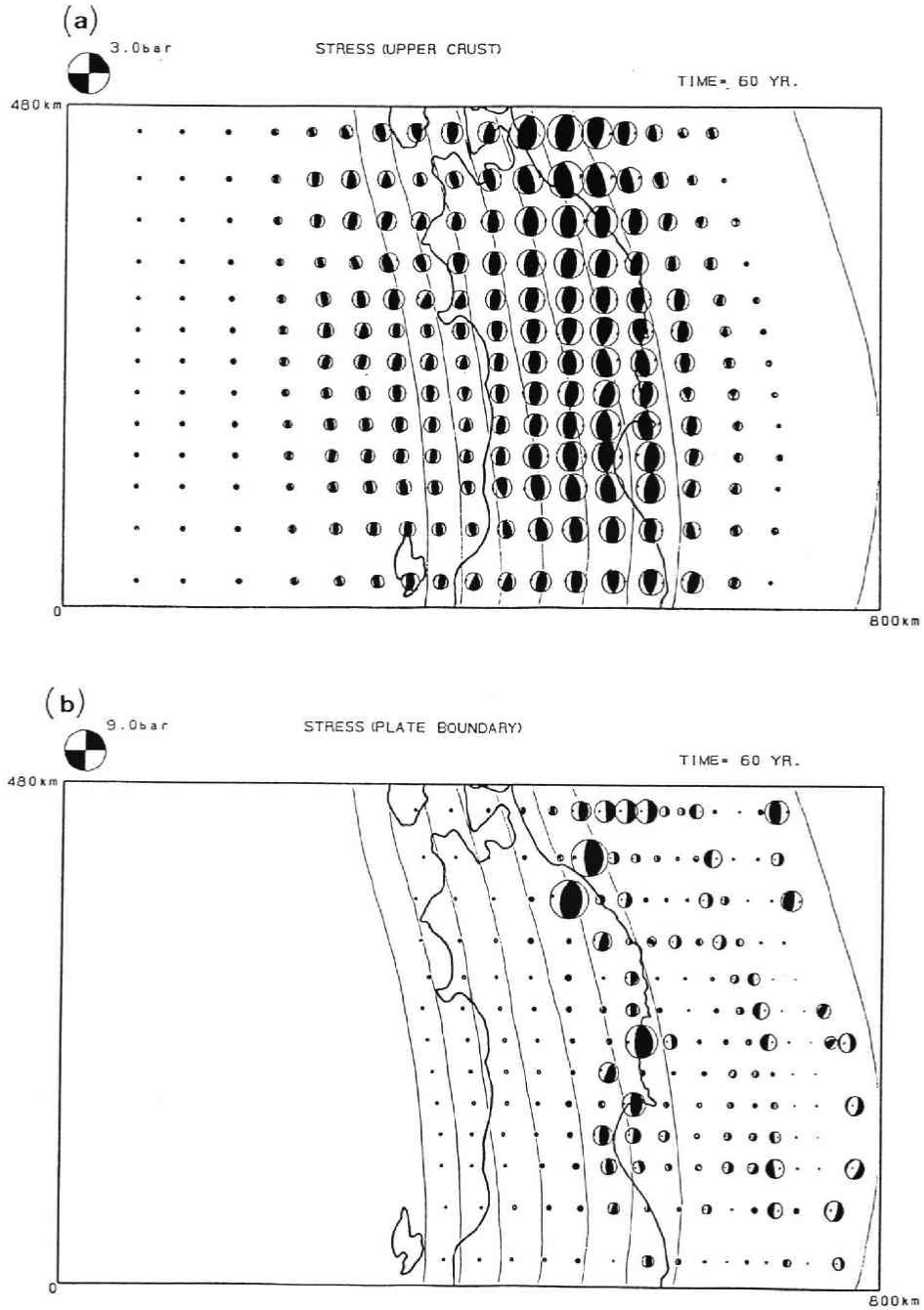

Fig. 26 The same as Fig. 20(a) and (b), but for the northern part model in the constant-coupling case.

respectively.

The profiles of the vertical displacements, for evample, along the segment I-I′ indicated in Fig. 13(a) are shown in Fig. 24. As clearly seen, there is in the land area a nodal point where no vertical movement occurs throughout the whole time sequence. This is consistent with the results obtained by Sato (1980) and Miura (1982), although its position is somewhat different. Observations also suggest existence of such nodes in the land area (Miura, 1982).

Next we briefly look into the displacement vectors in vertical cross-section. Fig. 25 shows those at 60 years in the vertical cross-section along the segment I-I′ in the constant-coupling case. Although the displacement arising from dragging by the subducting Pacific slab is predominant, patterns of the vectors are different among those in the eastern and western portions of the cross-section. The vectors seem to rotate clockwise with respect to a point near the Japan Sea coast on the earth's surface. Such general feature of the displacement vectors is found in other cases where the prescribed displacements on the coupling interface are uniform.

5.2.2 Stress Field

Here we again show and discuss the stress field in the northern part model mainly on the bases of those at the time step of 60 years as in the case of the southern part model.

The stresses in the upper crust and in the portion just above the interface of the subducting Pacific slab are presented in Figs. 26(a) and (b), respectively, for the case of the constant seismic-coupling. In the land area, the stresses in the upper crust have almost same magnitude, that is, a few bars. They have almost horizontal compression axes nearly in east-west direction. Such orientation of the compressional axis is manifestation of the compression by the subducting Pacific plate and is consistent with the results obtained by observations (*e.g.* Nakamura and Uyeda, 1980).

The stresses in the portion which is about 100 km away to the east from the Pacific coast are, however, extremely small. This may be of no significance, being merely due to the boundary conditions. But if not so, it should be possible to consider the reason for this as follows: in this portion, the compressional stress is regarded, in a qualitative sense, to be cancelled more or less by the tensional stress arising from bending of the overriding plate including the crust itself. Such a zone, where the stresses are extremely small, may correspond to the 'aseismic belt' proposed by Yamashina *et al.* (1977), although its position is somewhat easterly compared with that of this belt. They also considered the same reason or the existence of the belt as that regarded here.

The stresses at far off shore of the Japan Sea coast are very small. This means that the compressional force due to the subduction of the Pacific plate does not transmit efficiently to the back arc region.

The stress field along the plate interface is not so systematic as that in the upper crust. The stresses Just beneath the coastal line of the Pacific ocean are remarkably large at some regions. They are different from those inferred from seismic activities. Thus such a stress field as shown in Fig. 26(b) seems not to be actual one.

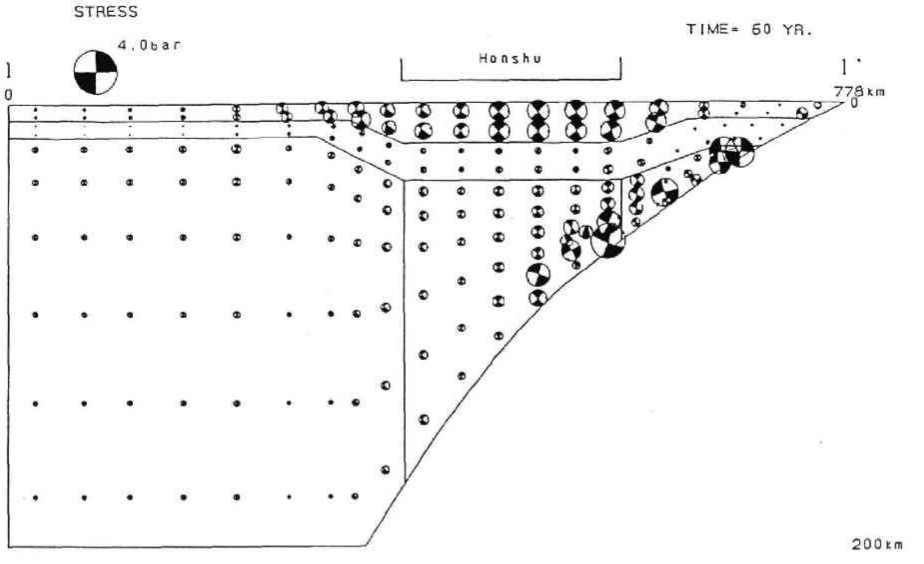

Fig. 27 The same as Fig. 21, but for the northern part model in the constant-coupling case. This cross-section is along the segment I-I' in Fig. 13(a).

As an example of stress distributions in vertical cross-sections, the one in the cross-section along the segment I-I' is shown in Fig. 27. It should be noted that the stresses are exprssed as the front hemisphere projections. The contrast in magnitudes of stresses between those in the upper and lower crusts is strikingly clear. The stresses in the upper crust are large, whereas those in the lower crust are very small. Such distribution of stresses in the crust is consistent with the seismic activity pattern shown in Fig. 4 (Takagi *et al.*, 1977). The stress distribution along the plate boundary is, however, inconsistent with the seismic activity pattern within this portion.

To improve the stress distribution along the plate boundary, we carried out calculations for the case-(a) and case-(b) where the prescribed displacements are not homogeneous. The results are presented in Figs. 28(a) and (b) for the case-(a) and case-(b), respectively.

In the case-(a), stresses are extremely large in the vicinity of the trench axis which corresponds to the shallower portion along the plate boundary.

In the case-(b), on the contrary, stresses are relatively large at the western half of the region between the trench axis and the Pacific coast. This portion corresponds to the deeper part of the plate boundary. The belt like zones lying off the Pacific coast in both cases, where the stresses are very small, correspond to the lower crust, where the stresses are relaxed enough. Such features of the stress distribution patterns in both cases may be more clearly understood when those in vertical cross-sections are displayed as shown in Figs. 29(a) and (b).

By comparing the obtained stress fields with the distribution pattern of large earthquakes shown in Fig. 6 (Hasegawa *et al.*, 1985), it is readily supposed that the case-

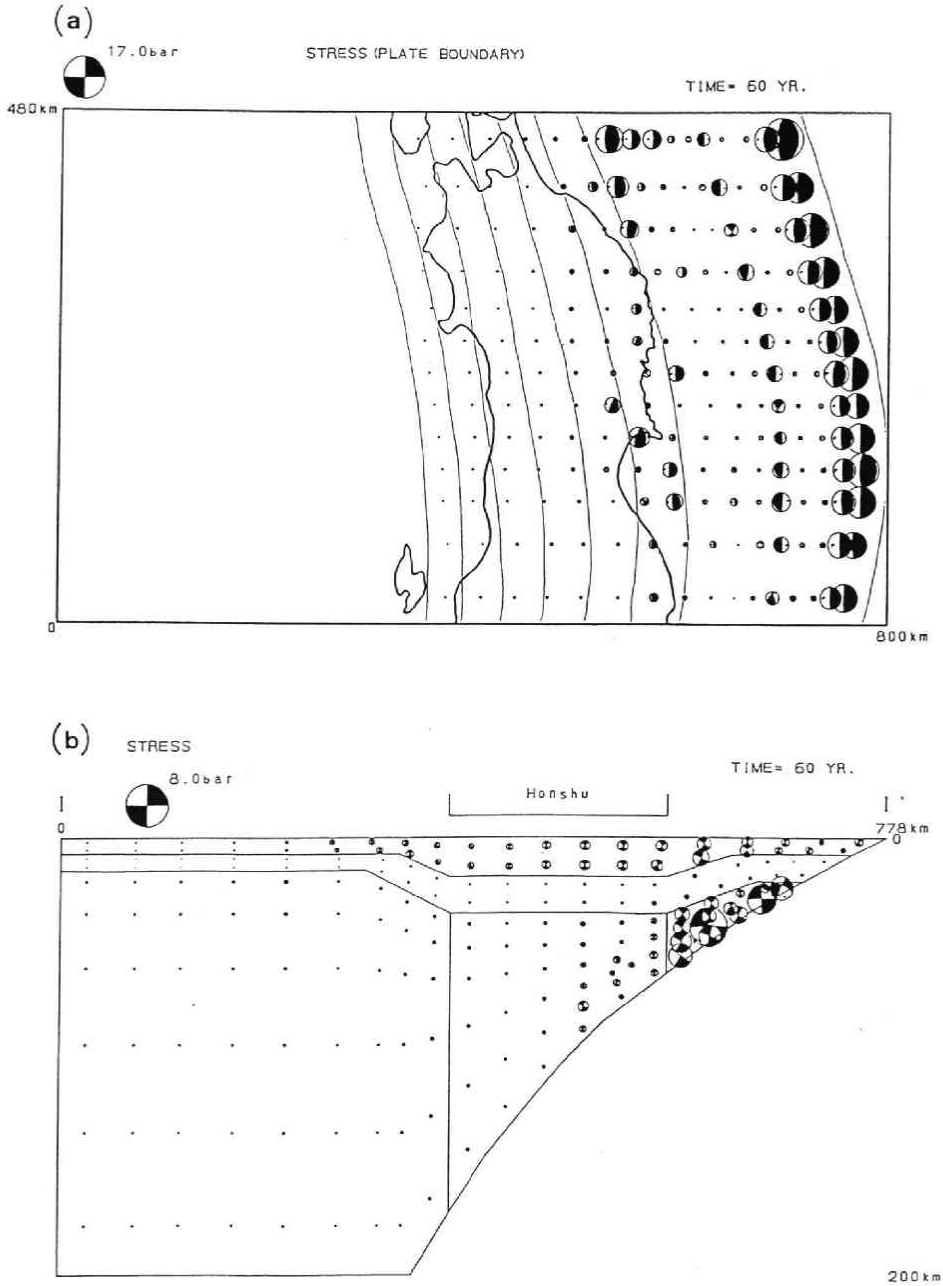

Fig. 28 Three-dimensional stresses along the plate boundary between the Pacific plate and overriding plate obtained for the northern part model in the case-(a) (a) and case-(b) (b), respectively. Notations are the same as in Fig. 20.

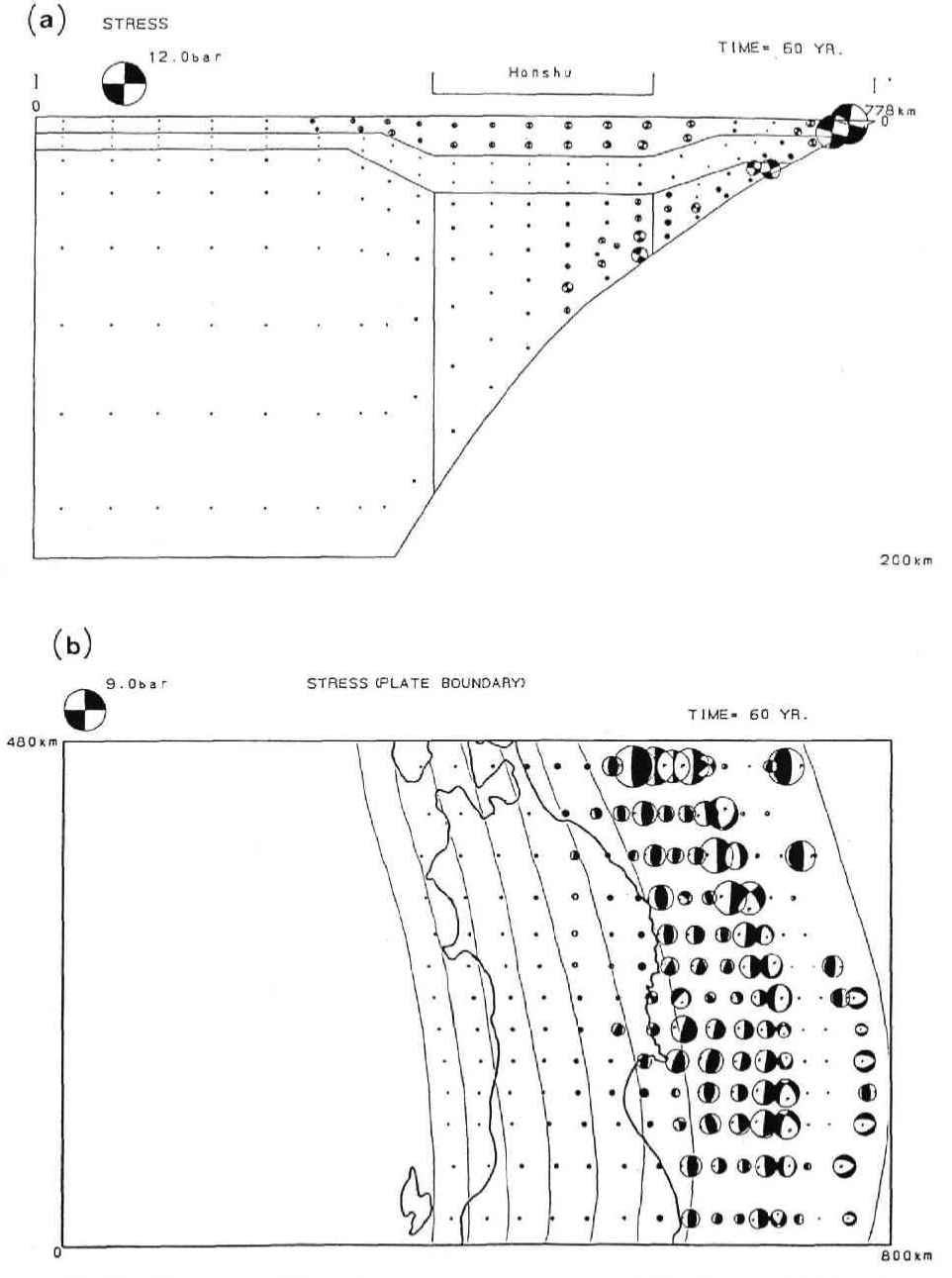

Fig. 29 The same as Fig. 21, but for the northern part model in the case-(a) (a) and case-(b) (b)respectively.

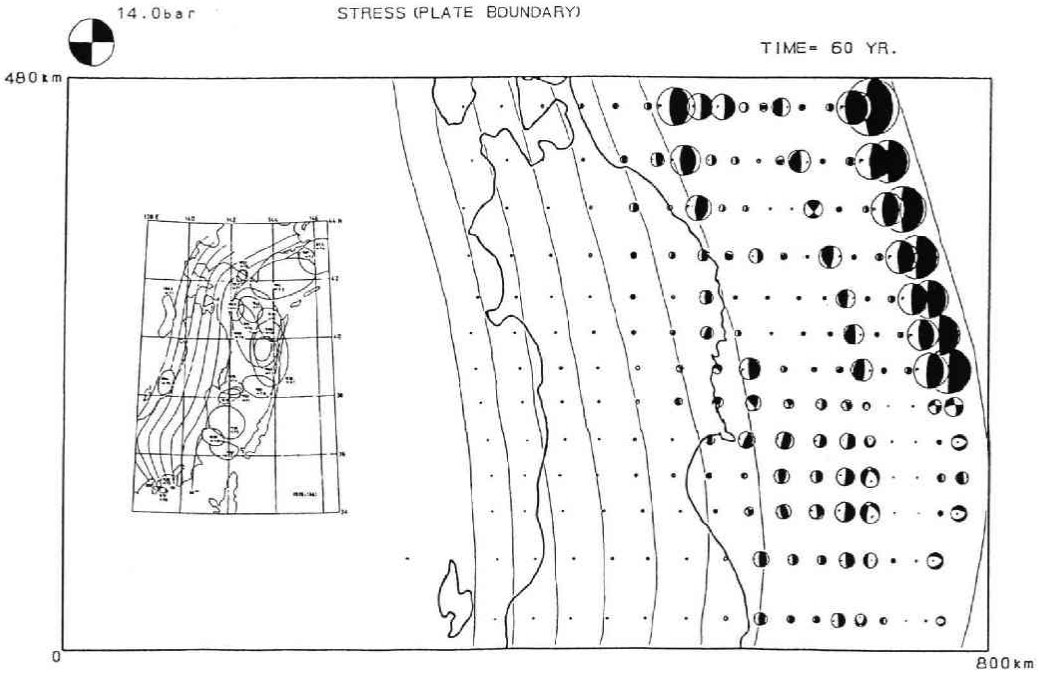

Fig. 30 The same as Fig. 28, but in the case-(c), where the boundary coditions for the case-(a) and case-(b) are combined.

(a) and case-(b), respectively, correspond to the northern and southern portions of the region between the trench axis and the Pacific coast. These portions are bordered by latitude line of about 38°N. Thus a further calculation is made for the case-(c), where the variations in the magnitudes of the prescribed displacements upon the plate interface are combined in the above sense.

The stress distribution thus obtained along the plate boundary is shown in Fig. 30. Correspondence between the distribution of calculated stresses and that of large earthquakes is regarded to be fairly good. Therefore, it seems reasonable to consider that the coupling factor, *i.e.*, a parameter to denote the strength of the seismic-coupling between the underthrusting oceanic plate and the overriding land side plate, may vary spatially in the northern and southern portions, for example, as those in the case-(a) and case-(b), respectively.

6. Discussion

6.1 Precision of Results

In order to simulate the crustal movements and states of stresses in and around the northeastern Japan island arc, we have calculated the displacement and stress fields by using three-dimensional visco-elastic finite element method. For the sake of simplicity, we divided the arc into the southern and northern parts and made calculations for each part separately.

First we should point out some practical problems which we are forced to face in the calculations. In the finite element analyses, it is very important to pay much attention to the element divisions in order to ensure high precision in calculations. The size and shape of each element should be as small and uniform as possible, and consequently, the numbers of nodes and elements should be as large as possible. However, we could not satisfactorilly do so because of the limited capacity of the current computer. The smallest element in our models is about 20 km×20 km×20 km in dimensions, which is not necessarily sufficient for precise calculations.

Irregularities in the sizes and/or shapes of elements possibly affect the precisions of the calculated displacement and stress fields. Hence the obtained displacement and stress fields should be contaminated to some extent due to such problems related to the element divisions. This contamination may amount to about 10 to 20% of the magnitude of each displacement or stress in the worst case.

Furthermore, the larger the numbers of the nodes and elements are, the longer the cpu time is. This is another restriction to ensure high precision in the visco-elastic analyses, because we could not shorten the time increments in these analyses less than 20 years. Nevertheless, the results obtained in this study may still preserve some characteristic patterns, so that they can contribute to a certain extent to make clear the tectonics of the northeastern Japan island arc.

Next mentioned are the effects of the so-called fixed-conditions (*i.e.*, the boundary conditions that no displacement is allowed in certain directions). Such conditions may introduce artificial boundaries into the models. Then the stresses in the vicinity of such boundaries tend to be extremely large. Such stresses seem to be far from the actuality. Thus we should reduce the effects of the artificial boundaries. One of the possible ways for the purpose is to use the 'infinite domain elements' proposed by Beer and Meek (1981). Improved modeling by using this kind of elements will be made in the future.

Besides such practical difficulties, there are ambiguities in constructing the models due to lack of our knowldege on the underground structures and interactions between the subducting and overriding plates.

6.2 Underground Structures and Material Properties

For the southern part, underground structure and material properties are not well established because of its complexity. In our model of this part, not only the overriding land side plate but also the descending oceanic slabs of the Pacific and Philippine-Sea plates are included. In such a model, it may be better to introduce boundary layers between the overriding and subducting plates. The layers are considered to be transitional ones and partially melted, having smaller rigidity and viscosity.

We may be able to control the strength of seismic-coupling between two plates by changing the rigidities and/or viscosities of these boundary layers. We, however, did not introduce such boundary layers because their detailed characteristics are not well known in spite of some authors' suggertions on the possible existence of them (*e.g.* Okada, 1979; Hurukawa and Hirahara, 1980; Hashimoto, 1981).

Thus instead of incorporating the boundary layers into the model, we imposed the prescribed velocities upon the oceanic slabs whose magnitudes are only one-third of the plate velocities themselves. This is approximately equivalent to assign the seismic-coupling factors equal to 0.3 (*i.e.*, 30%).

A large discrepancy between the calculated and observed vertical displacements as shown in subsection 5.1.1, however, seems to suggest that the seismic-coupling in this region may be much weaker than that indicated by this value. Another explanation for the discrepancy is that the overriding and subducting plates may be decoupled with each other nearly completely at most portion of the plate interface. Only at a little portion they may be partially coupled with each other. Such partially coupled portion is considered to correspond to a seismically active region (or the so-called earthquake nest) remarkably identified in the Kanto district (*e.g.* Takemoto and Kawasaki, 1983).

It is very important to investigate quantitatively the seismic-coupling between the overriding and subducting plates, because it directly affects the displacement and stress fields within the overriding plate or in the vicinity of the plate boundary. We should, therefore, extend the study on this problem in the future.

Material property of each sub-region is also not well known. In particular, viscosities are most controversial. Several authors have estimated viscosity distribution in the earth's mantle based upon the data of postglacial uplifts in the regions such as the Fennoscandia and arctic Canada (*e.g.* Haskell, 1935; Takeuchi and Hasegawa, 1964; Walcott, 1973; Cathles, 1975; Peltier and Andrews, 1976; Peltier, 1976). Their results show that viscosity in the upper mantle is of the order of 10^{22} poise, and it decreases to about 10^{20} poise in the depth between about 100 and 200 km.

Referring to these estimates, we assigned a homogeneous viscosity of 4×10^{22} poise to the asthenosphere in the southern part model. In the case of the northern part model, we assigned inhomogeneous viscosities varying from 10^{20} poise to 10^{22} poise to the asthenosphere by taking account of the Q-structure presented by Umino and Hasegawa (1983). The lower value is based upon the viscosity given by Thatcher and Rundle (1979) and Thatcher *et al.* (1980). On the other hand, we assumed much lower viscosity of 10^{18} poise for the lower crust based on Yamada (1973).

The viscosity of each sub-region, however, seriously affects the stress state by controlling the stress relaxation rate. Thus the values of the viscosities used in the present study should be modified in the future, if rheological characteristic of each region is better established.

6.3 Boundary Conditions on Plate Boundary

We consider herein the boundary conditions which should be imposed upon the plate interface between the Pacific plate and overriding plate in the case of the northern part model. The boundary conditions should be given so that they can simulate the interaction between these two plates as realistically as possible. However, little knowledge on the interaction between the subducting and overriding plates is available at present. We must, therefore, try to calculate under various types of boundary conditions consider-

ing the observed facts such as the distribution of large earthquakes, their recurrence times and the speed of plate motion.

One of the most fundamental problems related to such boundary conditions is that which is better to be imposed upon the plate interface, stress or displacement. In other words, it is to be judged which type of boundary condition can represent more realistically the actual interactions between the subducting and overriding plates. Several researchers consider that the strength of seismic-coupling between these plates at their interface can be expressed by the ratio of the amount of seismic slip rate to the speed of relative motion between the plates concerned with (*e.g.* Abe, 1977 ; Kanamori, 1977 ; Takemoto and Kawasaki, 1983 ; Kawasaki and Matsuda, 1987). Furthermore, it is considered that the seismic slip rate is roughly equal to the interseismic displacement rate of the overriding plate, which is dragged into depth by the subducting plate at their interface. We can, therefore, estimate the magnitude of displacement which should be imposed upon the plate interface, provided that the strength of the seismic-coupling is known or assumed. Thus, in order to control the strength of the seismic-coupling, it seems to be much direct to give displacement as the boundary condition.

On the contrary, there is no direct estimation of shear stress exerted on the plate interface by the subducting plate. There are only some indirect ones for some subduction zones (*e.g.* Froidevaux and Isacks, 1984 ; Honda, 1985 ; Furukawa and Uyeda, 1986). According to them, the magnitude of the shear stress at plate interface varies from about 100 to 1000 bars. Thus it is difficult to determine exactly it. Therefore, we chose the boundary conditions of displacement type to be imposed upon the plate interface. However, for comparison, an example of results obtained under the stress-boundary-conditions will be referred to later.

It is, next, a basic problem how the strength of the seismic-coupling should be quantitatively determined or assumed because it directly affects the stress and displacement fields within the overriding plate, particularly, in the vicinity of the plate interface. According to the investigations by Abe (1977), Kanamori (1977), Takemoto and Kawasaki (1983) and Kawasaki and Matsuda (1987), the strength of the seismic-coupling, namely the coupling factor, between the subducting oceanic plates and overriding land side plate is estimated to be about 0.2 to 0.3 (or 20% to 30%) in and around the Japan island arc. Thus we adopt the value of 0.3 for it, although it may vary slightly around this value from one region to another.

In order to consider spatial variations of the coupling factor we took account of the distiribution pattern of large earthquakes, because this factor is considered to be large in the regions where large eathquakes frequently occur, while small in other regions. It is, however, difficult to determine quantitatively its variation, even if its qualitative behavior is thus presumable.

Hence we assumed exponential variations of this factor as represented by the expressions (1) and (2) in subsection 4.2.2. In these cases, the coupling factors vary from 80% to 120% of their mean values. We also calculated the stress and displacement fields by using the coupling factors which vary from 90% to 110% or from 100% to 110% of

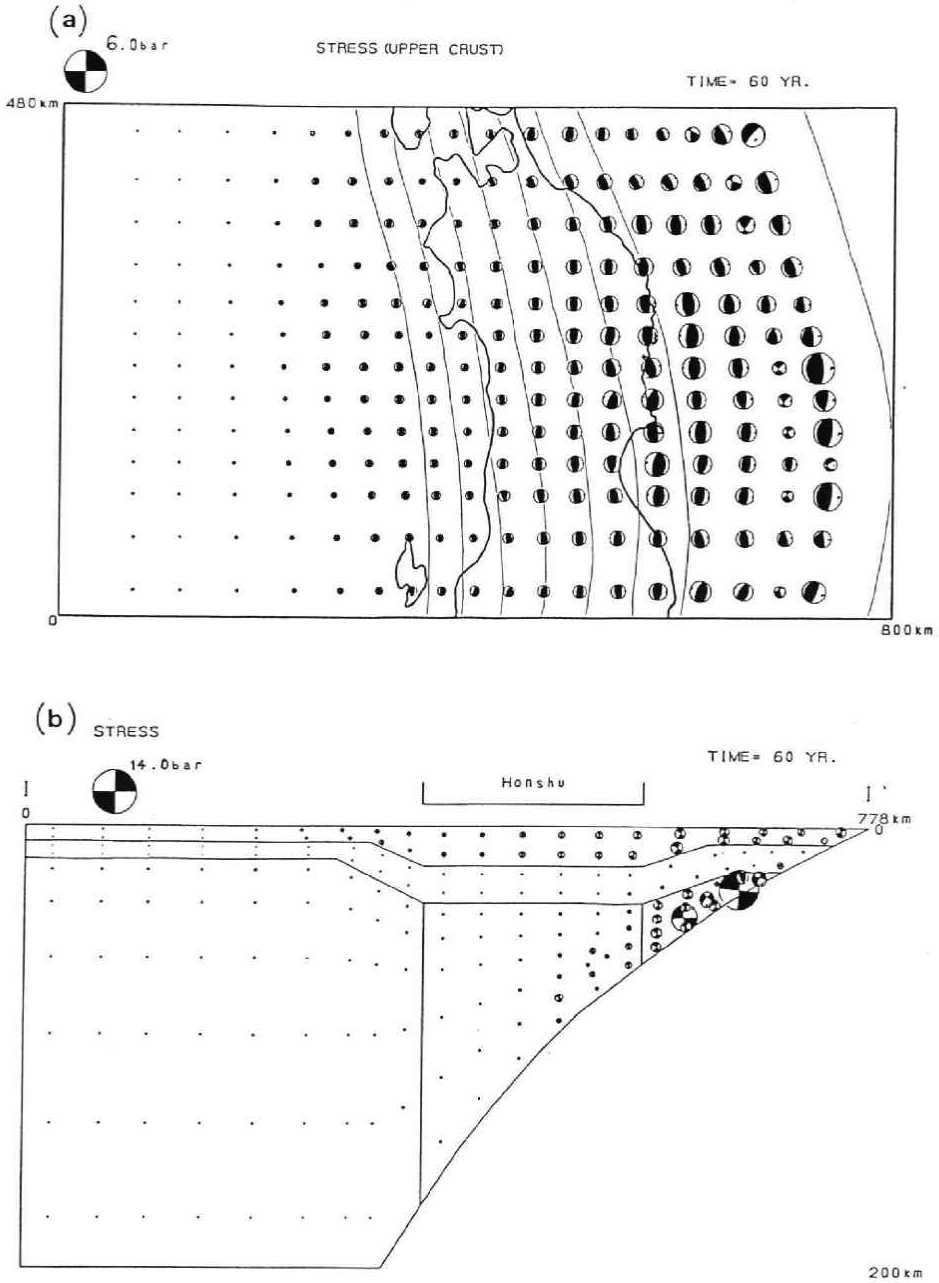

Fig. 31 Three-dimensional stresses in the upper crust projected onto the lower hemispheres (a), and in the vertical cross-section along the segment I-I' in Fig. 13 (a) projected onto the front hemispheres (b), respectively. These are obtained for the northern part model in the case of stress-boundary-condition at the time of 60 years. Notations are the same as in Fig. 20.

their mean values. The results of these calculations are, however, not appreciably different from those presented in section 5.2. Therefore, the results described there are considered to be representative ones for the case of exponentially varying couplig factor.

Finally we briefly mention the results obtained under a stress-boundary-condition. Figs. 31(a) and (b), respectively, show the states of stresses in a horizontal plane (upper crust) and vertical plane (cross-ssection along the segment I-I' in Fig. 13(a)) at the time of 60 years. We imposed a uniform shear stress upon the plate interface between the trench axis and the position just beneath the aseismic front.

By comparing these figures with Figs. 26(a) and 27 which are obtained under the constant displacement-boundary-condition, we find a few differences. First, in the case of the stress-boundary-condition, the position with the largest stress is relatively easterly, and the stresses within the upper crust beneath the land area gradually decrease as it becomes westerly. Second, the stresses in the portion which is about 100 km away to the east from the Pacific coast are not small in contrast with those obtained under the displacement-boundary-condition. This may imply that, in the case of the stress-boundary-condition, compressional stress arising from thrusting by the Pacific plate is not so effectively cancelled by tensile stress associated with under-bending of the overriding plate as in the case of the displacement-boundary-condition.

7. Conclusions and View for Further Study

We calculated the displacement and stress fields caused by plate interactions in and around the northeastern Japan island arc by using three-dimensional finite element method. Since this arc is considered to be composed of two quite different structures, namely the southern and northern parts, we divided it into these two parts, and made calculations separately. These two parts roughly correspond to the Kanto and Tohoku districts, respectively.

Main results for the southern part are as follows.

(1) The direction of horizontal displacement at the earth's surface almost coincides with that of the Pacific plate motion in the eastern half region and with that of the Philippine-Sea plate motion in the western half region.

(2) The vertical displacement field at the earth's surface is characterized by a remarkable subsidence at the northern portion of the Kanto plain. Although the rate of the calculated subsidence is about five times larger than the observed rate, the pattern of this subsidence has a striking resemblance to the so-called Kanto basin building (*e.g.* Naruse, 1968).

(3) Stresses are very large in and around the portion where the two oceanic plates are colliding with each other, *i.e.*, the region of slab-slab collision, as well as those in shallower portion of the plate boundary between the subducting and overriding plates. This characteristic in the stress distribution is consistent with the stress pattern generating large earthquakes in these portions along the plate interface.

(4) The stress field in crust beneath the land area is revealed to be almost horizontally compressional. This is nearly consistent with the one summarized by Tsukahara

and Ikeda (1983).

On the other hand, main results for the northern part are as follows.

(1) The pattern of observed vertical movement with a remarkable subsidence in the Pacific ocean side and with a slight uplift in the Japan Sea side is reproduced by the calculations. However, the nodal line at which no vertical movement occurs lies somewhat westerly compared with the one estimated by Miura (1982).

(2) The stresses in the land area have almost horizontal and east-west direction of compressional axes. The stress field is consistent with the results summarized by Nakamura and Uyeda (1980). The stresses in the upper crust increase with time more rapidly than those in the lower crust. Such behaviors of the stresses in the upper and lower crusts beneath the land area well interpret the observed seismicity.

(3) The distribution pattern of large earthquakes beneath the Pacific ocean may be interpreted by considering a spatial variation in the strength of the seismic-coupling between the subducting slab and overriding plate: we obtained a stress field which can explain this pattern by considering seismic-coupling factors decreasing and increasing, respectively, exponentially with the distance from the trench axis for the northern and southern areas bordered by a latitude line of about 38°N.

The precision of the calculation is, however, not always satisfactory both in the senses of time and space because we could not make the models sophisticated enough and the time increment in visco-elastic analyses short sufficiently due to the limited ability of the current computer. Thus more precise calculation is desirable in the future, if such restrictions would be reduced.

On the other hand, at present, we do not have enough knowledge which is needed for construction of models as realistically as possible on such points as the plate geometry, underground structures, material properties and how the plates interact each other. Much progress in researches on these points should be made.

In addition to improvement of each modeling, it is also very important to expand the model so that the entire Japan island arc is included within one model as already proposed by Kono (1985). It will be possible to simulate simultaneously many geophysical phenomena in and around the Japan island arc by using such a large scale model. To achieve the simulation successfully, first of all, more precise investigation on each region must be carried out one by one.

Furthermore, migrations of strain and tilt reported by some researchers (*e.g.* Ishil *et al.*, 1978, 1980; Kasahara, 1973; Yamada, 1973) are also very interessing and important phenomena. Thus simulations of them, which we did not concern with in the present study, are very desirable in the future in order to promote our understanding of the physics in subduction zones.

Acknowledgements: The author would like to express his hearty gratitude to Prof. A. Takagi for helpful guidance and encouragement throughout the course of this study. He is much indebted to Profs. T. Hirasawa and H. Hamaguchi for their invaluable suggestions and discussions in the study. Drs. A. Hasegawa, K. Yamamoto and S. Horiuchi are

gratefully acknowledged for their useful advice. Thanks are also due to Prof. H. Ishii, Dr. K. Yamazaki, Mr. S. Miura and all the members of the Observation Center for Prediction of Earthquakes and Volcanic Eruptions of Tohoku University for their kind advice and assistance. This study were made for the degree of Doctor of Science at Tohoku University. Computations in this study were mainly made at the Computer Center of Tohoku University.

References

Abe, K., and Kanamori, H., 1970: Upper mantle structure of the Philippine Sea, in *Island Arc and Ocean* (edited by M. Hoshino, and H. Aoki), Tokai Vniv. Press, Tokyo, 85-91.

Abe, K., 1977: Tectonic implications of the large Shioya-Oki Earthquake of 1938, *Tectonophys.*, **41**, 269-289.

Aoki, H., 1974: Plate tectonics of arc-junction at central Japan, *J. Phys. Earth*, **22**, 141-161.

Beer, G., and Meek J. L., 1981: 'Infinite domain' elements, *Inter. J. Num. Meth. Eng.*, **17**, 43-52.

Bird, P., 1978: Finite element modeling of lithospheric deformation: The Zagros collision orogeny, *Tectonophys.*, **50**, 307-336.

Bischke, R.E., 1974: A model of convergent plate margins based on the recent tectonics of Shikoku, Japan, *J. Geophys. Res.*, **79**, 4845-4857.

Cathles, L.M.III, 1975: Viscosity of the earth's mantle, Princeton Univ. Press, Princeton, 386 pp.

Dambara, T., 1971: Synthetic vertical crustal movements in Japan during the recent 70 years, *J. Geod. Soc. Japan*, **17**, 100-108 (in Japanese).

Forsyth, D., and Uyeda, S., 1975: On the relative importance of the driving forces of plate motion, *Geophys. J. R. astr. Soc.*, **43**, 163-200.

Froidevaux, C., and Isacks, B.L., 1984: The mechanical state of the lithosphere in the Altiplano-Puna segment of the Andes, *Earth and Planet. Sci. Lett.*, **71**, 305-314.

Furukawa, Y., and Uyeda, S., 1986: Thermal state under Tohoku arc with consideration of crustal heat generation, *J. Volcan. Soc. Japan*, **31**, 15-28 (in Japanese).

Goto, K., Hamaguchi, H., and Suzuki, Z., 1985: Earthquake generating stresses in a descending slab, *Tectonophys.*, **112**, 111-128.

Harada, T., and Isawa, N., 1969: Horizontal deformation of the crust in Japan — Result obtained by multiple fixed stations —, *J. Geod. Soc. Japan*, **14**, 101-105 (in Japanese).

Hasegawa, A., Umino, N., and Takagi, A., 1978: Double-planed structure of the deep seismic zone in the northeastern Japan arc, *Tectonophys.*, **47**, 43-58.

Hasegawa, A., Umino, N., Takagi, A., Suzuki, S., Motoya, Y., Kameya, K., Tanaka, K., and Sawada, Y., 1983: Spatial distribution of earthquakes beneath Hokkaido and northern Honshu, Japan, *Zisin*, **36**, 129-150 (in Japanese).

Hasegawa, A., Umino, N., and Takagi, A., 1985: Seismicity in the northeastern Japan arc and seismicity patterns before large earthquakes, *Earthq. Predict. Res.*, **3**, 607-626.

Hashimoto, M., 1981: Three-dimensional stress distribution in southwestern Japan as expected from the configuration of the subducting Philippine Sea plate (Part 2), *Zisin*, **34**, 197-211 (in Japanese).

Hashimoto, M., 1984: Finite element modeling of deformations of the lithosphere at an arc-arc junction: The Hokkaido corner, Japan, *J. Phys. Earth*, **32**, 373-398.

Hashimoto, M., 1985: Finite element modeling of the three-dimensional tectonic flow and stress field beneath the Kyushu island, Japan, *J. Phys. Earth*, **33**, 191-226.

Haskell, N.A., 1935: The motion of a viscous fluid under a surface load, *Physics*, **6**, 265-269.

Honda, S., 1985: Thermal structure beneath Tohoku, northeast Japan — A case study for understanding the detailed thermal structure of the subduction zone, *Tectonophys.*, **112**, 69-102.

Horii, K., and Kawahara, M., 1970: A numerical analysis on visco-elastic structures by the finite element method, *Proc. Japan Soc. Civil Eng.*, **179**, 23-35 (in Japanese).

Hurukawa, N., and Hirahara, K., 1980: Structure of the Philippine Sea plate subducting beneath the Kii peninsula, *Zisin*, **33**, 303-316 (in Japanese).

Ishida, M., 1986: The configuration of the Philippine Sea and the Pacific plates as estimated from

the high-resolution microearthquake hypocenters in the Kanto-Tokai district, Japan, *Rep. Nation. Res. Cent. Disas. Prevent.*, **36**, 1-19 (in Japanese).

Ishii, H., Sato, T., and Takagi, A., 1978 : Characteristics of strain migration in the northeastern Japan arc (I) — Propagation characteristics —, *Tohoku Geophys. J.*, **25**, 83-90.

Ishii, H., Sato, T., and Takagi, A., 1980 : Characteristics of strain migration in the northeastern Japan arc (II) — Amplitude characteristics —, *J. Geod. Soc. Japan*, **26**, 17-25.

Ishii, H., Komukai, Y., and Takagi, A., 1981 : Characteristics of vertical land movement and microearthquake activity in the northeastern Japan arc, *Tectonophys.*, **77**, 213-231.

Jungels, P.H., and Frazier, G.A., 1973 : Finite element analysis of the residual displacements for an earthquake rupture ; Source parameters for the San Fernand Earthquake, *J. Geophys. Res.*, **78**, 5062-5083.

Kanamori, H., and Press, F., 1970 : How thick is the lithosphere ?, *Nature*, **226**, 330-331.

Kanamori, H., 1977 : Seismic and aseismic slip along subduction zones and their tectonic implications, in *Island Arcs, Deep Sea Trenches and Back-Arc Basins* (edited by M. Talwani and W.C. Pitman III), *A.G.U. Maurice Ewing Ser.*, **1**, 163-174.

Kasahara, K., 1973 : Earthquake fault studies in Japan, *Phil. Trans. R. Soc. Lond.*, **A274**, 287-296.

Kasahara, K., 1975 : Aseismic faulting following the 1973 Nemuro-Oki Earthquake, Hokkaido, Japan (a possibility), *Pure Appl. Geophys*, **113**, 127-139.

Kasahara, K., 1985 : Patterns of crustal activity associated with the convergenece of three plates in the Kanto-Tokai area, central Japan, *Rep. Nation. Res. Cent. Disas. Prevent.*, **35**, 33-137 (in Japanese).

Kato, T., 1979 : Crustal movements in the Tohoku district, Japan, during the period 1900-1975, and their tectonic implications, *Tectonophys.*, **60**, 141-167.

Kawasaki, I., and Matsuda, K., 1987 : Interplate seismic coupling in south Kanto district, central Japan, and the hypothetical Tokyo Earthquake, *Zisin*, **40**, 7-18 (in Japanese).

Kobayashi, Y., 1983 : Commencement of the plate "subduction", *Chikyu*, **3**, 510-518 (in Japanese).

Kono, Y., 1985 : The Japanese Island Simulator (JIS) Project, in Panel Discussion "Present Status and Future Scope of the Research on Crustal Movement", *J. Geod. Soc. Japan*, **31**, 149-152 (in Japanese).

Kosloff, D., 1977 : Numerical simulations of tectonic processes in southern California, *Geophys. J. R. astr. Soc.*, **51**, 487-501.

Maki, T., Kawasaki, I., and Horie, A., 1980 : Earthquake mechanisms associated with the conjunction of the sinking plates beneath the Kanto district, central Japan, *Bull. Earthq. Res. Inst. Univ. Tokyo*, **55**, 577-600.

Maki, T., 1984 : Focal mechanisms and spatial distribution of intermediatedepth earthquakes beneath the Kanto district and vicinity with relation to the double seismic planes, *Bull. Earthq. Res. Inst. Univ. Tokyo*, **59**, 1-51.

Minamino, T., and Fujii, N., 1981 : The effect of the contorted "nose" of a subducting slab on the stress field in the continental lithosphere at an arc-arc junction, *Geophys. J. R. astr. Soc.*, **67**, 143-158.

Minster, J.B., and Jordan, T.H., 1978 : Present-day plate motions, *J. Geophys. Res.*, **83**, 5331-5354.

Minster, J.B., and Jordan, T.H., 1979 : Rotation vectors for the Philippine and Rivera Plates, *EOS Trans. Am. Geophys. Un.*, **60**, 958.

Miura, S., 1982 : Study on the characteristics of crustal movements and seismotectonics in the northeastern Japan arc, M.Sc. thesis, Tohoku Univ. (in Japanese).

Mogi, K., 1985a : Tectonic singularities of the epicentral region of the 1983 Japan Sea Earthquake, *Zisin*, **38**, 262-265 (in Japanese).

Mogi, K., 1985b : 1983 Japan Sea Earthquake (M7.7) and seismotectonics in northeastern Japan, *Bull. Earthq. Res. Inst. Univ. Tokyo*, **60**, 401-428 (in Japanese).

Nakamura, K., and Uyeda, S., 1980 : Stress gradient in arc-back arc regions and plate subduction, *J. Geophys. Res.*, **85**, 6419-6428.

Nakamura, K., 1983 : Possible nascent trench along the eastern Japan Sea as the convergent boundary between Eurasian and north American plates, *Bull. Earthq. Res. Inst. Univ. Tokyo*, **58**, 711-722 (in Japanese).

Naruse, Y., 1968 : Quaternary crustal movements in the Kanto region, *Memoirs Geol. Soc. Japan*, **2**, 29-32 (in Japanese).

Noguchi, S., 1985: The configuration of the Philippine Sea plate and characteristics of seismicity in the Ibaraki region, *Chikyu*, **7**, 97-104 (in Japanese).

Ohtake, M., and Takahashi, H., 1982: Contribution of the down-hole observation of crustal activity to earthquake prediction, *Proc. Intern. Symp. Continental Seismicity and Earthquake Prediction*, Beijing.

Ohtake, M., and Kasahara, K., 1983: Paired earthquake in the Ibaraki region, central Japan, *Zisin*, **36**, 643-653 (in Japanese).

Okada, H., 1979: New evidences of the discontinuous structure of the descending lithosphere as revealed by ScSp phase, *J. Phys. Earth*, **27**, suppl., S53-S63.

Peltier, W.R., 1976: Glacial-isostatic adjustment-II. The inverse problem, *Geophys. J. R. astr. Soc.*, **46**, 669-705.

Peltier, W.R., and Andrews, J.T., 1976: Glacial-isostatic adjustment-I. The forward problem, *Geophys. J. R. astr. Soc.*, **46**, 605-646.

Research Group for Explosion Seismology, 1977: Regionality of the upper mantle around northeastern Japan as derived from explosion seismic observations and its seismological implications, *Tectonophys.*, **37**, 117-130.

Sato, K., 1980: Study on the seismotectonics in the northeastern Japan arc, M. Sc. thesis, Tohoku Univ. (in Japanese).

Sato, K., Ishii, H., and Takagi, A., 1981: Characteristics of crustal stress and crustal movements in the northeastern Japan arc (I): Based on the computation considering the crustal structure, *Zisin*, **34**, 551-563 (in Japanese).

Seno, T., 1977: The instantaneous rotation vector of the Philippine Sea plate relative to the Eurasian plate, *Tectonophys.*, **42**, 209-226.

Seno, T., 1979: Intraplate seismicity in Tohoku and Hokkaido and large interplate earthquakes: A possibility of a large interplate earthquake off the southern Sanriku coast, northern Japan, *J. Phys. Earth*, **27**, 21-51.

Shimazaki, K., 1974: Pre-seismic crustal deformation caused by an underthrusting oceanic plate, in eastern Hokkaido, *Phys. Earth Planet. Inter.*, 8, 148-157.

Shimazaki, K., Nakamura, K., and Yoshii, T., 1982: Complicated pattern of the seismicity beneath metropolitan area of Japan: Proposed explanation by the interactions among the superficial Eurasian plate and the subducted Philippine Sea and Pacific slabs, *Abstr. paper presented at Intern. Conf. Mathem. Geophys.*, Chateau de Bonas, France, Terra cognita, **2**, 403.

Takagi, A., Hasegawa, A., and Umino, N., 1977: Seismic activity in the northeastern Japan arc, *J. Phys. Earth*, **25**, suppl., S95-S104.

Takagi, A., 1985: Seismo-Tectonics of Arc-Trench System in the Northeastern Japan, J. Geod. Soc. Japan, **31**, 124-146.

Takemoto, H., and Kawasaki, I., 1982: Seismic coupling between the Philippine Sea and the Eurasian plates in the Kinugawa area, the southwestern part of Ibaraki prefecture, central Japan, *Zisin*, **36**, 531-539 (in Japanese).

Takeuchi, H., and Hasegawa, Y., 1964: Viscosity distribution within the earth, *Geophys. J. R. astr. Soc.*, **9**, 503-508.

Thatcher, W., and Rundle, J.B., 1979: A model for the earthquake cycle in underthrust zones, *J. Geophys. Res.*, **84**, 5540-5556.

Thatcher, W., Matsuda, T., Kato, T., and Rundle, J.B., 1980: Lithospheric loading by the 1896 Riku-u Earthquake, northern Japan: Implications for plate flexure and asthenospheric rheology, *J. Geophys. Res.*, **85**, 6429-6435.

Togawa, H., 1979: A guide book to the finite element method, Saiensu-sya, Tokyo, 174 pp (in Japanese).

Togawa, H., 1981: Introduction to the finite element method, Baifu-kan, Tokyo, 324 pp (in Japanese).

Tsukahara, H., and Ikeda, R., 1983: State of stress in the Kanto-Tokai area, *Zisin*, **36**, 571-586 (in Japanese).

Umino, N., and Hasegawa, A., 1975: On the two-layered structure of deep seismic plane in northeastern Japan arc, *Zisin*, **28**, 125-139 (in Japanese).

Umino, N., and Hasegawa, A., 1983: Qs structure beneath northeastern Japan, *Ann. Meet. Seismol.*

Soc. Japan Absir., **1**, 53 (in Japanese).
Uyeda, S., and Sugimura, A., 1970: The island arcs, Iwanami, Tokyo, 156 pp (in Japanese).
Walcott, R.I., 1973: Structure of the earth from glacio-isostatic rebound, in *Ann. Rev. Earth Planet. Sci.*, 1 (edited by F.A. Donath), Ann. Rev. Inc., Palo acto, 15-37.
Yamada, J., 1973: A water-tube tiltmeter and its application to crustal movement studies, *Special Bull. Earthq. Res. Inst. Univ. Tokyo*, **10**, 1-147 (in Japanese).
Yamashina, K., Shimazaki, K., and Kato, T., 1977: Aseismic belt in island arc, *Ann. Meet. Seismol. Soc. Japan Abstr.*, **1**, 75 (in Japanese).
Yoshii, T., 1975: Proposal of the "Aseismic Front", *Zisin*, **28**, 365-367 (in Japanese).
Zienkiewicz, O.C., 1977: The finite element method (3rd. ed.), McGraw-Hill, Berkshire, 787 pp.